# Biomimetic Surfaces and their Effect on Bacterial Attachment, Adhesion and Retention

J H SPALL

2019

# BIOMIMETIC SURFACES AND THEIR EFFECT ON BACTERIAL ATTACHMENT, ADHESION AND RETENTION

**Joshua Spall**

**A Thesis submitted in fulfilment of the requirements of the Manchester Metropolitan University for the degree of Master of Science (by Research)**

**School of Healthcare Sciences**
**Manchester Metropolitan University**
**2019**

## Contents

## Index of Figures

**Index of equations**



This thesis would have not been possible without the support from the micro team at MMU, my family, Dexter and Professor Kathryn Whitehead, who knows the difference between a carrot and a stick.

**Abstract**

Biofouling in the dairy industry accounts for billions of dollars in lost product each year. Surface properties, such as macro, micro and nano topography and hydrophobicity were analysed with bacteria in monoculture and co-culture to determine the surface characteristics that prevented biofilm formation. Replica biomimetic surfaces were made using dental wax from five different types of plant leaves (White Cabbage (*Brassica oleracea capitate*), Leek (*Allium ampeloprasu*), Tender Heart (*Brassica oleracea*), Cauliflower *(Brassica oleracea var. botrytis*), and Gladioli (*Gladiolus*); this included a flat surface wax control. Surface physicochemistry was determined using contact angle measurements and surface topography ($S_a$, $S_q$, and $S_{pv}$) using optical profilometry. Monoculture and co-culture bacterial attachment, adhesion and retention assays were carried out using *Escherichia coli* and *Listeria monocytogenes* and determined using colony-forming units/mL. Scanning Electron Microscopy provided quantitative cell counts (CFU/cm$^2$). The results demonstrated that the Tenderheart leaf surface was the most hydrophobic with the highest surface free energy, highest $\gamma_s^{AB}$, most electron-donating and most electron-accepting surface. The Leek surface demonstrated the lowest surface free energy. The White cabbage surface was the most non-polar surface, with the least $\gamma_s^{AB}$ properties, the least electron-accepting and least electron-donating surface. However, it had the highest $S_a$ and $S_q$ values. The Cauliflower leaf surface was the least hydrophobic and least nonpolar surface whilst the Gladioli surface was found to have the highest $S_{pv}$ values. Finally, the flat surface showed the lowest $S_a$, $S_q$ and $S_{pv}$ values. Following the attachment, adhesion and retention assays, *E. coli* in monoculture did not show any trends between the surface properties and the number of cells retained. However, for *L. monocytogenes* in monoculture, following the attachment and retention assays the Flat surface showed the least number of cells (6 $Log_{10}$ CFU/cm$^2$ and 4.5 $Log_{10}$ CFU/cm$^2$ respectively). Following

the adhesion and retention assays, the Gladioli surface (highest $S_{pv}$ values) displayed the lowest numbers of *L. monocytogenes* cells (6 $Log_{10}$ CFU/$cm^2$ and 3.7 $Log_{10}$ CFU/$cm^2$ respectively). Use of the bacteria in co-cultures demonstrated that for both the attachment and retention assays, the Tenderheart surface (most hydrophobic) displayed the lowest number of cells (4.5 $Log^{10}$ CFU/$cm^2$ and 3.4 $Log^{10}$ CFU/$cm^2$ for *E. coli*, 5.1 $Log_{10}$ CFU/$cm^2$ and 3.9 $Log_{10}$CFU/$cm^2$ for *L.monocytogenes* respectively). SEM analysis did not correlate with the CFU/mL assays. However, with *L. monocytogenes* the flat surfaces (lowest roughness) retained the lowest numbers of cells (4.7 $Log_{10}$ cells /$cm^2$) and regarding the co-culture, the White cabbage surface (most hydrophilic) displayed the lowest number of cells when tested for bacterial attachment, adhesion and retention (4.1 $Log_{10}$ cells /$cm^2$, 4.5 $Log_{10}$ cells /$cm^2$ and 0 $Log_{10}$ cells /$cm^2$ respectively. These results demonstrate that when more topographically complex surfaces are analysed, the conclusions drawn between the effect of the surface properties on bacterial attachment, adhesion and retention from more uniform surfaces do not apply. Further, the processes of bacterial attachment, adhesion and retention are different and hence differentiation between these classifications needs to be clarified. It became apparent that the varying methods used produced a wide range of results and that the use of different bacteria in monoculture and co-culture affected the microbial assays. Hence, a new approach needs to be taken to understand the cell: surface interactions on complex surfaces.

## Introduction

Biofouling is a major concern in many different industries. The dairy industry must prevent biofouling not only to stop product wastage but also to avert the distribution of contaminated product that can cause transmission of bacteria to consumers (Fu *et al*., 2016). Biofouling in the dairy industry accounts for billions of dollars in lost product each year. Causes of this include protein denaturation, protein aggregation and bacterial fouling (Bansal and Chen, 2006).

Most of these industries rely on physical cleaning such as washing down dairy equipment regularly with cleaning products or clean in place procedures (Guozhen *et al*., 2019). Modern methods of bacterial removal are either chemical or physical. Physical removal methods can consist of the use of steam or pressure, ultraviolet light exposure and manual scrubbing. Chemical removal methods can consist of the use of sodium hypochlorite, sodium hydroxide and novel methods such as bacteriocins, bacteriophages, essential oils, non-thermal plasma and quorum sensing inhibitors (Fister *et al*., 2016; Galié *et al*., 2018).

In the UK outbreaks transmitted by food occur multiple times a year, often linked with raw drinking milk or improper handling of meat (Pennington, 2014). In 2016, an outbreak within mixed salad leaves resulted in the transmission of a strain of *Escherichia coli* to 161 people throughout England Scotland and Wales, with 62 of the patients needing hospital care. Unfortunately, this outbreak resulted in the death of two patients (Gobin et al., 2018).

In 2017, a total of 135 cases of Listeriosis were reported in England and Wales of which 30.3% of patients died (Public Health England, 2018). Removing bacteria from industrial equipment is a costly process that results in equipment downtime, for example in the paper industry downtime and breakdowns caused by bacterial build-up can cost between $2000 and $10,000 in every instance (Bajpai, 2015). A possible method to prevent food spoilage is to prevent initial bacterial attachment and subsequent biofilm formation. The application

of biomimetic topographies may provide a solution to stop bacterial accumulation on surfaces in the food industry (Shahali *et al*., 2019).

**Biomimetic surfaces**

Biomimetic surfaces are created to replicate all or some of the properties of surfaces found in nature, such as macro, micro and nano topography, unique surface structures and chemical interactions (Hwang *et al*., 2015). Biomimetic surfaces can be produced by many different methods. The use of photolithography is a common method due to its high level of detail (Boyan *et al*., 2017). The process of creating a biomimetic surface with photolithography starts with analysing a bioLogical surface with microscopy and extracting detailed X, Y and Z spatial data, which is then used to create a greyscale digital photomask. A UV light is applied to a surface coated with a photoresist layer which uses the mask as a template. The surface is developed with a solvent to remove material from the surface leaving the etched pattern behind (Kyle *et al*., 2016). These methods require specific equipment throughout making them cost-intensive and so not suited to the large-scale production. Fabrication via a mould is an alternative option which is far more cost-effective without compromising detail on the microscale (Wiedemeier *et al*., 2017). In more recent years 3D scanning and printing have become a far more economical alternative to biomimetic surface production. Multiple sets of quantitative surface characteristic data can be obtained with magnetic resonance imaging, topography analysis and ultrasound. This data gives information about the surface and the structure below that can be printed as individual layers with a resolution up to 50nm (Xiao *et al*., 2019; Vaidya and Solgaard, 2018).

**Properties of leaf surfaces**

The surface of some plant leaves have unique properties that allow them to repel debris that has settled on their surface. The most well known of this phenomenon is the Lotus effect. Lotus leaves and many other similar Nelumbonaceae have papillae on each epidermis cell on the adaxial side. These are narrow structural protrusions coated in epicuticular wax that minimize water to leaf contact area increasing surface hydrophobicity. The papillae's primary functions concerning hydrophobicity are to increase surface area and protect the epicuticular wax (Ensikat *et al*., 2011). Water contact pressure also determines how the surface reacts to liquid; rain droplets travelling at an average speed of 3 m/s would on a more ridged surface carry enough energy to protrude into the sub-papillae air pockets thus negating the structural hydrophobicity (Koch *et al*., 2008). However, due to the flexibility of the leaf itself the impact energy is absorbed and so the water droplet rolls off (Ensikat *et al*., 2011). Surface wettability is measured by analysing the contact angle of water on a surface. A surface with a water contact angle <90° is considered wettable and a surface with a contact angle >90° is considered non-wettable, any surface with a water contact angle >150° is considered superhydrophobic (Law, 2014).

The epicuticular wax is the principal component of the surface's hydrophobicity, if it is removed the leaf contact angle reduces from 161°to 122° consequently lowering its status from superhydrophobic to non-wettable. The epicuticular wax is thought to be the most crucial component in plant leaf composition concerning bacterial attachment (Marcell and Beattie, 2002).

**Topography and bacteria**

The relationship between microbial attachment and surface topography is dependent on multiple variables ($S_a$, $S_q$ and $S_{pv}$). Surface topography can be divided into three main categories representing the size of surface variation, nano (< 0.5 µm), micro (>0.5 µm – 10 µm) and macro (<10 µm) (Rajab *et al*., 2017). Due to the presence of multiple roughness

structures on the leaf surface, any contaminating particles are carried away with the water droplets resulting in a self-cleaning surface (Yamamoto *et al*., 2015).

Topographies of manufactured surfaces can vary greatly depending on the method of production, surfaces with an average peak to valley height ($S_a$) that is similar to specific bacterial cell size may retain more of that species bacteria than surfaces with a much smaller or larger $S_a$. Bacterial morphology also influences retention, rod-shaped cells may not become trapped in any surface features or pits due to their elongated shape compared to cocci bacteria (Whitehead and Verran, 2006).

Nano topography has been shown to influence bacterial adhesion, by altering a glass surface, resulting in a more wettable surface (44.8°- 41.6°), decreased $S_a$ (2.1-1.3 mm) and other surface parameters. A three-factor reduction in adhered cells was observed per $mm^2$ (Mitik-Dineva *et al*., 2008). Macroscopic topography variations have been shown to provide a preferential position for initial bacterial deposition from the surrounding medium (Lorenzetti *et al*., 2015).

**Surface Topography in nature**

Papillae and waxes exist in nature to primarily prevent fouling of the plant and water loss (Barthlott *et al*., 2017). “Bioinspired” surfaces have been developed that take inspiration from nature replicating topographical features such as nano spikes, nanowires, and nano grass, that use these features to create a bactericidal environment. The surfaces replicated cicada and dragonfly wings and gecko skin (Tripathy *et al*., 2017). Each surface had a wide variation of wettability and bactericidal efficacy. Some of the surfaces created were observed rupturing the cell wall in what is known as the contact killing mechanism (Tripathy *et al*., 2017).

Sharkskin is coated in denticles situated micrometre apart from one another that move with the underlying elastic skin beneath. It is thought that the combination of the surface texture

and the denticle flexibility aids preventing bacterial attachment (Kesel and Liedert, 2007). A biomimetic surface called Sharklet has been developed mimicking shark skin microstructures and attributes with an aim to reduce bacterial attachment. Sharklet has been shown to reduce *E. coli* colony forming units (CFU) by 47% when compared to a smooth control surface concerning bacterial adhesion. A 77% reduction in colony size and an 80% reduction in migration were also reported when compared to the control surface (Reddy *et al*., 2011). It is thought that sharklet can do this due to its ability to put mechanical stress on bacterial cells that attempt to adhere to it. In a process called mechanotransduction surface structures create stress on the cell membranes when contact is made causing the cell to expend more energy to stay in contact with the surface thus making it disadvantageous to do so resulting in cell detachment (Schumacher *et al*., 2008). Sharklet is currently being applied in the medical industry for use in catheters and wound dressings (Magin *et al*., 2016).

**Surface Topography quantification**

Surface topography or roughness can be quantified in two separate ways, the measuring of one or more cross-sectional 2D lines drawn across the surface which is represented with the letter R when presenting values or 3D scanning which has recently become a more available alternative in which a map of the measured surfaces is digitally created and analysed. The types measurements remain the same as when looking at a 2D line or a 3D scan however they are represented with the letter R and S retrospectively. $R_a$ equal to the arithmetical mean height of a surfaces profile. However, if multiple $R_a$ measurements are made of the same surface then $R_a$ becomes indicative of the surface $S_a$ (Lancashire, 2017). $S_a$ is the most commonly used method of surface roughness quantification for quality control due to its ability to give a centre line average (CLA) and relative simplicity. It does not give information about surface wavelength and lacks the sensitivity to measure smaller surface

details. $S_q$ presents a parameter known as the surface Root mean square which describes the standard deviation of the distribution of surface heights. $S_q$ provides more accuracy when analysing large surface deviations when compared to $S_a$ (Gadelmawla *et al*., 2002). $S_{pv}$ is described as the total peak to valley height of a surface, this gives a general indication of surface roughness. However, it does not consider the shapes of surface details that form the overall roughness (Etxeberria *et al*., 2015). Surfaces designed to test bacterial affinity are typically uniform with structured peaks and troughs and so produce highly precise quantitative topographical data (Perera-Costa *et al*., 2014). BioLogical surfaces do not adhere to such strict architecture and so present a larger relative deviation in topographic analysis when compared to man-made surfaces (Scardino *et al*., 2009).

**Physicochemistry of surfaces**

The hydrophobicity of a surface is directly related to its wettability. Many factors affect surface wettability such as surface chemistry and micro and nano topography (Härth and Schubert, 2012);(Duta *et al*., 2015). Surface wettability is determined by the mean left and right contact angle of a liquid placed on a surface. This data is analysed to determine the surface hydrophobicity which is presented in the form of the *ΔGiwi* (Van Oss, 1995). *ΔGiwi* is equal to the surface free energy ($\gamma_s$) of the sample (Barkai *et al*., 2016). *ΔGiwi* represents the amount to which a polar attraction between surface and water is greater or smaller than the polar attraction water molecules have between themselves. When the net free interaction energy between a surface and water is less than zero the surface is classed as hydrophobic, when interaction energy is greater than zero the surface is classed as hydrophilic. To obtain the *ΔGiwi* of a surface first the Lifshitz-Van der Waals surface energy ($\gamma_s^{LW}$) representing polar interactions and the Lewis acid-base surface energy ($\gamma_s^{AB}$) representing non-polar interactions must each obtained (Faten *et al*., 2016). Polar acid-base interactions are comprised of electron donor and acceptor interactions (Rosairo *et al*., 2001). Acid-base

interactions are typically due to electron donor ($\gamma_s^-$) and electron acceptor ($\gamma_s^+$) interactions. If a surface does not possess electron donor or acceptor then it is described as apolar, conversely, if it possesses both then it is described as bipolar (Chibowski, 1992).

**Surface Chemistry**

Epicuticular wax plays a crucial role in pathogen prevention in plants. Forming a smooth or crystalline layer on the external surface of plant leaves this wax is composed of very-long-chain aliphatics (Buschhaus *et al*., 2007). The composition and 3D structure of the wax creates a hostile environment in the pollysphere for bacteria. Select species of bacteria (*Bacillus* sp., *Janibacter* sp., *Kocuria* sp., *Methylobacterium* sp., *Microbacterium* sp., and Staphylococcus sp.) possess the ability to produce biosurfactants that degrade the Epicuticular wax, this grants them access to nutrients and water on the leaf surface bellow (Zeisler-Diehl et al., 2018; Siriratruengsuk et al., 2017).

***Escherichia coli***

*Escherichia coli* is a Gram-negative, rod-shaped, facultative anaerobic bacterium. Some *E. coli* strains form symbiotic relationships in humans and animals by aiding in the production of vitamin K and preventing pathogenic bacteria colonising the gastrointestinal tract (Lim *et al*., 2010). Other strains can cause outbreak and illness. Unpasteurised milk can act as a vector for the bacterium due to the faecal-oral transmission cycle of the bacteria and the location of udders in dairy animals (McClure and Hall, 2000). In 2016, the CDC reported that dairy accounted for 11% of all outbreaks in the US, although this figure represents only unpasteurized milk (CDC, 2016). In 1999, an outbreak was linked to *E. coli* present in pasteurized milk occurred in North Cumbria, UK and 114 people were affected, with 28 being admitted to hospital, resulting in the largest *E. coli* 0157 outbreak in England and Wales recorded at that time (Goh *et al*., 2002).

Enteric pathogenic *E. coli* infections can cause stomach cramps, bloody diarrhoea, fever and vomiting. *E. coli* 0157 has multiple virulence factors, one of which is the production of Shiga toxins which are bacteriophage encoded toxins that consist of an active subunit (A1) and five receptor binding subunits (B5). When bound to a host cell A1 is internalised into the cell cytoplasm where it inhibits cell protein synthesis, this can cause bloody diarrhoea or Haemolytic Uremic Syndrome (HUS) (Lim *et al*., 2010). *E. coli* can also produce heat-liable enterotoxin which stimulates membrane-bound adenylate cyclase in intestinal epithelial cells which leads to elevated levels of Cyclic adenosine monophosphate resulting in hypersecretion of electrolytes and water manifesting as diarrhoea in patients (Gyles, 1992).

***Listeria monocytogenes***

*Listeria monocytogenes* is a Gram-positive cocci bacterium in the firmicute family. It is a facultative anaerobe and is one of the most virulent foodborne pathogens (Chen *et al*., 2014). Listeriosis is most commonly contracted from contaminated animal products especially soft cheeses and unpasteurised milk (Hanson *et al*., 2019). Up to 30% of foodborne listeriosis cases in high-risk individuals such as the elderly and pregnant women can lead to meningoencephalitis, miscarriage or stillbirth and even death (Segado-Arenas *et al*., 2018). *L. monocytogenes* infects via the oral route, once inside the hosts intestine it enters the epithelial cells and targets the liver where it will begin to multiply. In healthy patients, this is commonly the final step of the infection as a cell-mediated immune response initiates and removes the cells. However, in immunocompromised patients, the infection will continue to spread from the liver to the blood with the possibility of host death (Ramaswamy *et al*., 2007).

*L. monocytogenes* contamination in the food industry is relatively common due to its virulence factors, it is a facultative halophile and can grow in temperatures as low as 0°C.

It can be extremely difficult to remove from equipment, utensils, and floors in food production factories (Huang *et al*., 2016). Many aspects of the food industry operate at environmental temperatures between 4 and 12 °C when grown at this temperature *L. monocytogenes* displays a reduced affinity for biofilm formation (Bonaventura *et al*., 2008). At these temperatures *L. monocytogenes* biofilms displaying sparse clusters of cells and a reduced amount of EPS. (Colagiorgi *et al*., 2017).

**Microbial Co-cultures**

Mixed species biofilms are commonly found within the environment in which they often live in symbiosis and consequently enhancing the overall pathogenicity of clinically significant species (Madsen *et al*., 2012). Symbiosis can increase the biofilms virulence factors subsequently enhancing its proclivity for attachment (Camargo *et al*., 2017). Bacteria living in co-culture have been shown to have increased short-term mutation rates, increasing the possibility of antibiotic resistance (Frapwell *et al*., 2018). Co-culture biofilms have also been shown to present increased resistance to chemical agents such as chlorhexidine when compared to monoculture biofilms, this was due to shared protection conferred by neutralizing enzymes or inhibitory molecules that are spread throughout the biofilm (Marsh *et al*., 2011).

**Attachment, adhesion and retention**

Artificial surfaces commonly used in the food industry, such as polyethene, wood, glass rubber and stainless steel are subject to biofilm formation, this can lead to surface corrosion and alteration of product taste and smell (Galié *et al*., 2018). There are four stages of biofilm formation, attachment, adhesion, retention and biofilm development. Each stage making

bacterial removal more challenging. These stages can be affected by a multitude of environmental factors, such as bacterial species, surface roughness and surface hydrophobicity.

Bacterial attachment is the initial stage of interaction between bacterial cell and surface. This process is controlled primarily by two main processes, Brownian motion and Van der Waals forces. Brownian motion is described as the particles move throughout a medium allowing initial contact to be made (Marshall, 1986). Van der Waals forces are weak intermolecular forces that unlike covalent bonding do not rely on chemistry, instead, they rely on electron configuration to attract atoms (Yannopapas and Vitanov, 2007). Bacterial attachment as a result of van der Waals forces is a three-step process, the first employs Lifshitz–van der Waals forces which are effective over several hundred nanometres, the second step utilises Lifshitz–van der Waals forces in conjunction with electrostatic interactions which takes place at a distance of 20nm. The third step occurs at a distance of 5nm where specific cell receptors begin the process of adhesion. Throughout the stages of attachment, bacteria still present Brownian motion and can be removed by weak fluid shear forces (Palmer *et al*., 2007).

Bacterial adhesion creates a stronger bond between bacteria and surface. Bacterial adhesins are utilized to secure cells firmly to the structure. These adhesins can form part of bacterial appendages such as pili ad fimbriae. Multiple strains of *E. coli* poses P fimbriae which have the adhesin papG located at the fimbriae tip (Wullt, 2003). Multiple suggested theories are trying to fully explain the process of bacterial adhesion such as DVLO theory, Thermodynamic theory and Neuman's theory. An extended DVLO theory has been suggested that combines van der Waals forces, double layer interactions, acid-base interactions and hydrophobic interactions; however, this theory is not conclusive (Katsikogianni and Missirlis, 2004).

Bacterial retention becomes much more challenging due to bacterial cells utilizing surface topography and hydrophobicity, creating a more hospitable environment with the production of an extracellular polymeric matrix (EPS) (Bos *et al*., 2000; Donlan, 2002). This step of surface colonisation requires more physical force for bacterial removal to be achieved. Bacterial retention is the final step before biofilm formation (Whitehead et al., 2015). Due to the nature of bacterial attachment the longer cells are present on a surface the more mechanisms that are in place to prevent cell detachment such as adhesins and EPS formation (Pizarro-Cerda and Cossart, 2006).

This research aimed to determine the effects of bioinspired surface properties on bacterial attachment, adhesion and retention. Surface properties, such as macro, micro and nano topography and hydrophobicity were analysed with bacteria in monoculture and co-culture to determine the surface characteristics that prevented biofilm formation.

**Methods and materials**

Biomimetic replicates coupons emulating five different types of plant leaves (White Cabbage (*Brassica oleracea capitate*), Leek (*Allium ampeloprasu* ), Tender Heart (*Brassica oleracea*), Cauliflower *(Brassica oleracea var. botrytis*), and Gladioli (*Gladiolus*) and flat wax control were created by fabricating a silicone negative mould (Duosil silicone Shera; Germany) from the leaves by adhering them to a mould base with double-sided tape (3M). Dental wax (Kemdent Eco dental wax; UK) was poured into the negative mould creating a positive wax mould of each leaf. To create the individual coupons a 15 mm diameter steel hole punch (Trimming shop; UK) was used to create equally sized coupons.

Each biomimetic coupon was analysed with a goniometer (Krüss; Germany) using ultrapure water (BDH; UK), diiodomethane (Alfa Aesar; US) and formamide (VWR International;

US). A 5 µl drop of each liquid was applied to the surface. The left and right contact angle of the droplet was used to calculate the surface hydrophobicity with the Van Oss equation.

$$\Delta Giwi = -2\gamma_{iw} = -2\left[\begin{array}{l}((\gamma_i^{LW})^{1/2} - (\gamma_w^{LW})^{1/2})^2 + \\ 2\left((\gamma_i^+\gamma_i^-)^{\frac{1}{2}} + (\gamma_w^+\gamma_w^-)^{\frac{1}{2}} - (\gamma_i^+\gamma_w^-)^{\frac{1}{2}} - (\gamma_w^+\gamma_i^-)^{\frac{1}{2}}\right)\end{array}\right]$$

Equation 1. ΔGiwi equation (Van Oss, 1995)

**Surface Topography**

The coupons were measured with an optical light profilometer (Zygo; US) to find the $S_a$, $S_q$, and $S_{pv}$, a 3D scan of each surface was created and levelled to adjust for surface inclination. A surface cross-sectional line was also obtained from each surface. Images obtained with a maximum range of 160 µm x 160 µm in X and Y directions. For statistical analysis, three replicates for the same surface were measured five times each resulting in 15 measurements for each surface type.

**Bacterial preparation**

*E. coli* and/or *L. monocytogenes* were obtained from stock plates stored on tryptone soya agar (TSA) (Oxoid; US) at 4°C (Liebherr; Switzerland), placed into 10 mL of TSB and incubated for approximately 18 h at 37°C on an orbital shaker set at 150 rpm (New Brunswick Scientific; US). Cultures were then washed by centrifugation (Rotina 380, Hettich; Germany) at 1721 RCF three times, rinsing with sterile water in between. Cultures were diluted to an absorbance of 0.5 at 540nm on a spectrophotometer (+/- 10%) (Jenway; UK) equating to 3.38E+08 *E. coli* cells and 7.60E+08 *L. monocytogenes* cells per mL.

**Attachment (Wash) and Adhesion (Spray) assays**

The cell suspension was sprayed onto the biomimetic coupons using a compressed gas paint sprayer (Spraycraft; UK)for a duration of 5 s at a distance of 10 cm inside a class two laminar flow cabinet(Faster; Italy). Immediately after sterile distilled water was sprayed

onto the coupons for a duration of 5s at a distance of 10 cm. The spraying of both attachment and adhesion coupons was done in tandem, adhesion coupons were placed above the attachment as to prevent water dripping down and inadvertently washing them, both sets of coupons were adhered with double-sided tape in rows of four to a stainless steel tray which was angled at approximately 45°. The coupons from the spray assay were swabbed with 70% ethanol on their sides to remove residual bacteria. Each coupon was added to 2 mL of PBS (1 tablet per 100 mL)(Oxoid; US) and vortexed for one min. Coupons were extracted with sterile forceps and placed into a separate 2 mL of PBS and vortexed again. The contents of each of the two universals of PBS were then mixed, creating the solution to be used for serial dilutions. Each sample was diluted to $10^6$ in PBS by diluting at a ratio of 1:10. 3x10 µl drops were plated out from each dilution onto TSA, MacConkey agar (Oxoid; US) or oxford growth medium (Oxoid; US). The agar plates were incubated for 18 h at 37°C. A colony enumeration was then performed. The bacterial adhesion assay was methodologically very similar to the attachment assay except for the water rinse which did not occur.

**Retention assays**

Bacteria were prepared as in the bacterial preparation method. Each biomimetic coupon was submerged to 25 mL of solution for one hour at 37°C. Once incubated the cell suspension was poured off and 25 mL of sterile water was used to rinse the coupons. Each coupon was swabbed with 70% ethanol on the abaxial plane and its sides then added to 2 mL of PBS and vortexed for one minute, extracted with sterile forceps and placed into a separate two mL of PBS and vortexed again, each of the two universals of PBS were then mixed, creating the solution to be used for serial dilution. Samples were analysed as before.

In the case of monoculture assays, each experiment was run on TSA, however, for the co-culture analysis *E. coli* was grown on MacConkey agar and *L. monocytogenes* was grown on Oxford growth medium. Water controls were performed following the exact protocol of the assays previously stated with the only exception being the exemption of any bacteria.

**Scanning Electron Microscopy**

Throughout the multiple assay's samples were created in parallel and stored in 4% a glutaraldehyde (Agar Scientific, UK) solution then rinsed with sterile distilled water and dried for SEM analysis (Zeiss supra 40VT, Germany) to be used in conjunction with the CFU analysis. Three separate images were taken of each coupon; a cell enumeration was performed and used to ascertain the cells per $cm^2$. Images were analysed at a magnification of 5000x.

**Statistics**

Independent samples tests were used to compare all sets of data in individual categories, data was considered to be significant if $P=<0.05$. One way ANOVA and Kruskal-Wallis tests were used to compare all data collected. Statistical Product and Service Solutions (SPSS) was used to perform all statistical tests for this experiment.

## Results

### Surface Physicochemistry

The physicochemistry was carried out on the surfaces to determine the different surface free energy parameters of the surface topographies.

#### *Gibbs free energy (ΔGiwi)*

Analysis of the *ΔGiwi* results demonstrated that the results were not significantly different from one another. The Tenderheart surface (-3.6 *ΔGiwi* ) displayed as the least hydrophobic surface (Figure 1a) which was closely followed by the Cauliflower leaf surface (-9.9 *ΔGiwi*).

The Leek surface (-87 *ΔGiwi* ) and the White cabbage surface (-87.4 *ΔGiwi* ) presented as the most hydrophobic surfaces (Figure 1a). The Gladioli (-58.1 *ΔGiwi* ) and Flat (-65.1 *ΔGiwi*) surfaces appeared central in the range of data. Thus, the Tenderheart leaf surface was the most hydrophobic, whilst the Cauliflower leaf surface was the least hydrophobic.

#### *Surface free energy ($\gamma_s$)*

A significant difference was found when comparing the surface free energy of the White cabbage (37.7 $\gamma_s$) surface against the Leek (21.2 $\gamma_s$) (P= 0.028) and Flat (34.0 $\gamma_s$) (P=0.024) surfaces. The Tenderheart (67.6 $\gamma_s$) surface demonstrated the highest surface free energy value. The Gladioli (25.5 $\gamma_s$) surface displayed the second-lowest $\gamma_s$ value after the Leek surface. The Cauliflower *leaf* surface (40.8 $\gamma_s$) surface displayed the second-highest $\gamma_s$ value after the Tenderheart surface (Figure 1b). In summary, the Tenderheart leaf surface demonstrated the highest surface free energy whilst the Leek surface demonstrated the lowest surface free energy.

***Lifshitz-Van der Waals forces ($\gamma_s LW$)***

The White cabbage surface (37.4 $\gamma_s^{LW}$) when compared to the Gladioli surface (23.2 $\gamma_s^{LW}$) (P= 0.049) and the Cauliflower surface (15.9 $\gamma_s^{LW}$) (P= 0.033) showed a significant difference. The Flat surface (32 $\gamma_s^{LW}$) and the Tenderheart leaf surface (31.5 $\gamma_s^{LW}$) displayed with the second and third highest surface $\gamma_s^{LW}$. The Leek surface (21.0 $\gamma_s^{LW}$) displayed centrally in the range of data (Figure 1c). Hence, the White cabbage surface demonstrated the most non-polar surface, whilst the Cauliflower leaf surface demonstrated the least nonpolar surface.

***Lewis Acid-Base forces ($\gamma_s^{AB}$)***

No significant difference was found when surfaces were compared to one another. The Tender heart surface (36.2 $\gamma_s^{AB}$) and Cauliflower leaf surfaces (25.9 $\gamma_s^{AB}$) showed the highest Lewis acid-base value. The Leek (0.3 $\gamma_s^{AB}$), White cabbage (0.3 $\gamma_s^{AB}$), Gladioli, (2.3 $\gamma_s^{AB}$) and Flat (2.0 $\gamma_s^{AB}$) surfaces all displayed low values (Figure 1d). In summary, the Tenderheart plant surface demonstrated the highest $\gamma_s^{AB}$, whilst the White cabbage surface demonstrated the least $\gamma_s^{AB}$.

***Electron Acceptor ($\gamma_s^+$)***

No significant difference was found when comparing surface electron acceptor values ($\gamma_s^+$). The Tenderheart (15 $\gamma_s^+$) surface displayed the highest electron acceptor value, with the Cauliflower (14.1 $\gamma_s^+$) surface showing a slightly lower value. The Leek (0.2 $\gamma_s^+$) surface showed the lowest value, closely followed by the White cabbage (0.6 $\gamma_s^+$) surface. The Gladioli (3.0 $\gamma_s^+$) and Flat (2.0 $\gamma_s^+$) surfaces displayed relatively low values also (Figure 1e). Thus, the Tenderheart leaf surface was the most electron-accepting surface whilst the White cabbage surface was the least.

***Electron donor ($\gamma_s^-$)***

No significant difference was found when comparing surface electron donor values ($\gamma_s^-$). The Tenderheart (21.8 $\gamma_s^-$) surface displayed the highest electron donor values, which was followed by the Cauliflower (11.0 $\gamma_s^-$) surface. The Leek (0.1 $\gamma_s^-$), Gladioli (0.4 $\gamma_s^-$) and Flat (0.5 $\gamma_s^-$) surfaces displayed relatively lower values. The White cabbage (0.1 $\gamma_s^-$) surface displayed the lowest value (Figure 1f). In summary, the Tenderheart leaf surface was the most electron-donating, whilst the White cabbage surface was the least.

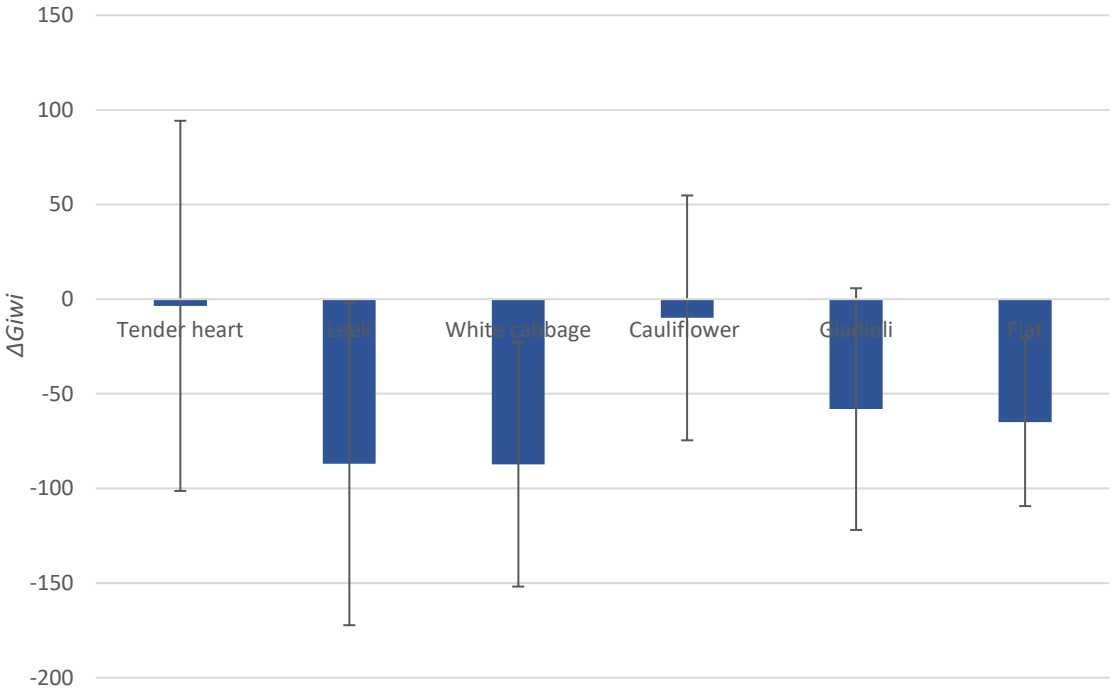


1a) ΔGiwi

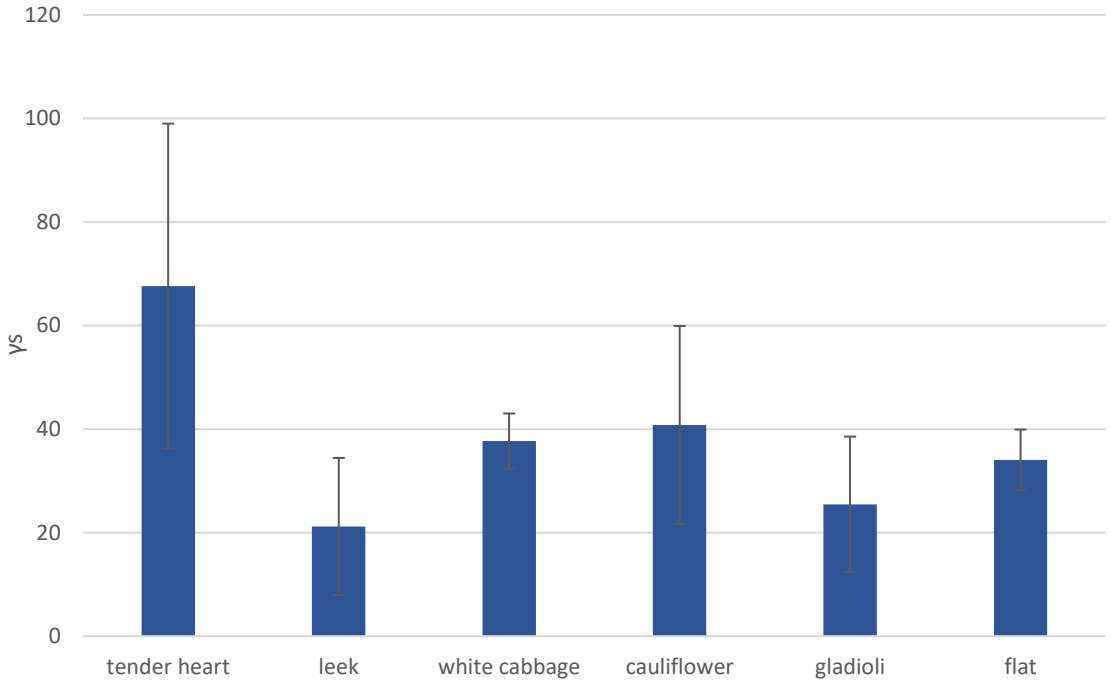


*1b)* surface free energy

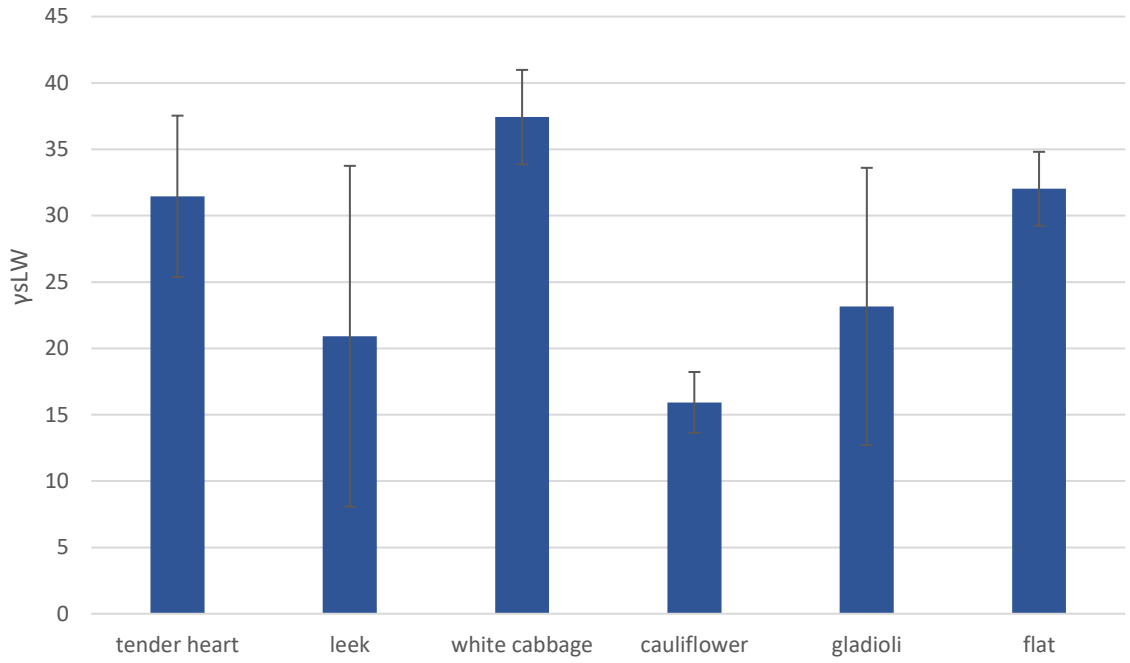


*1c)* Lifshitz-van der Waals

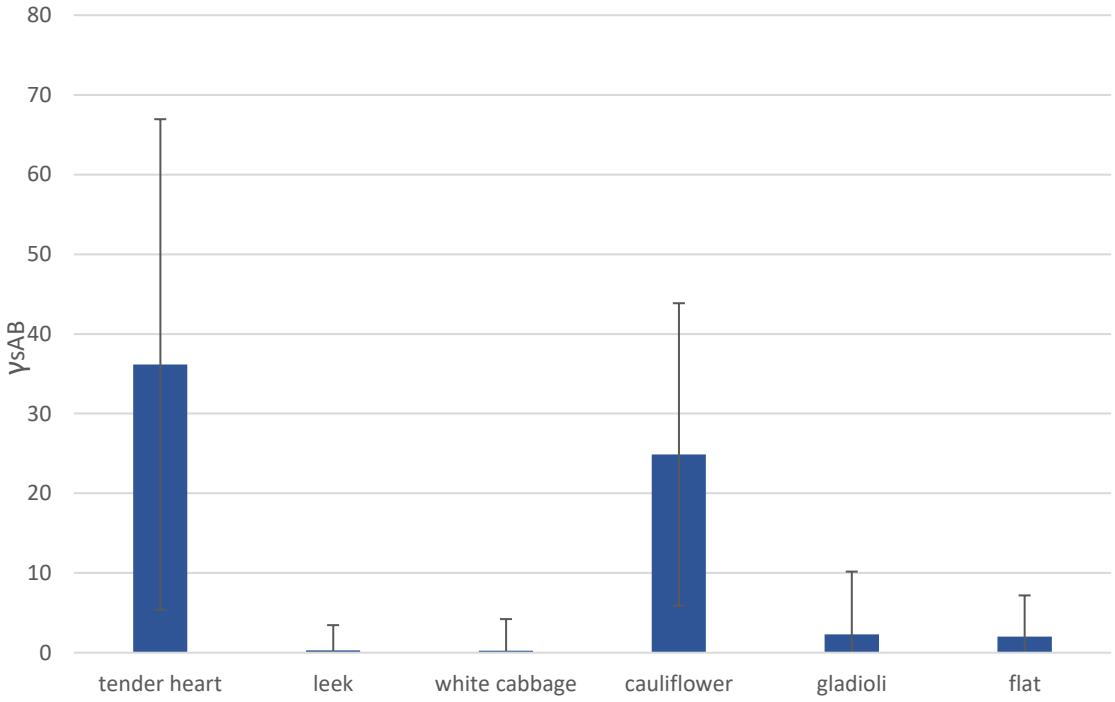


*1d)* Lewis acid-base

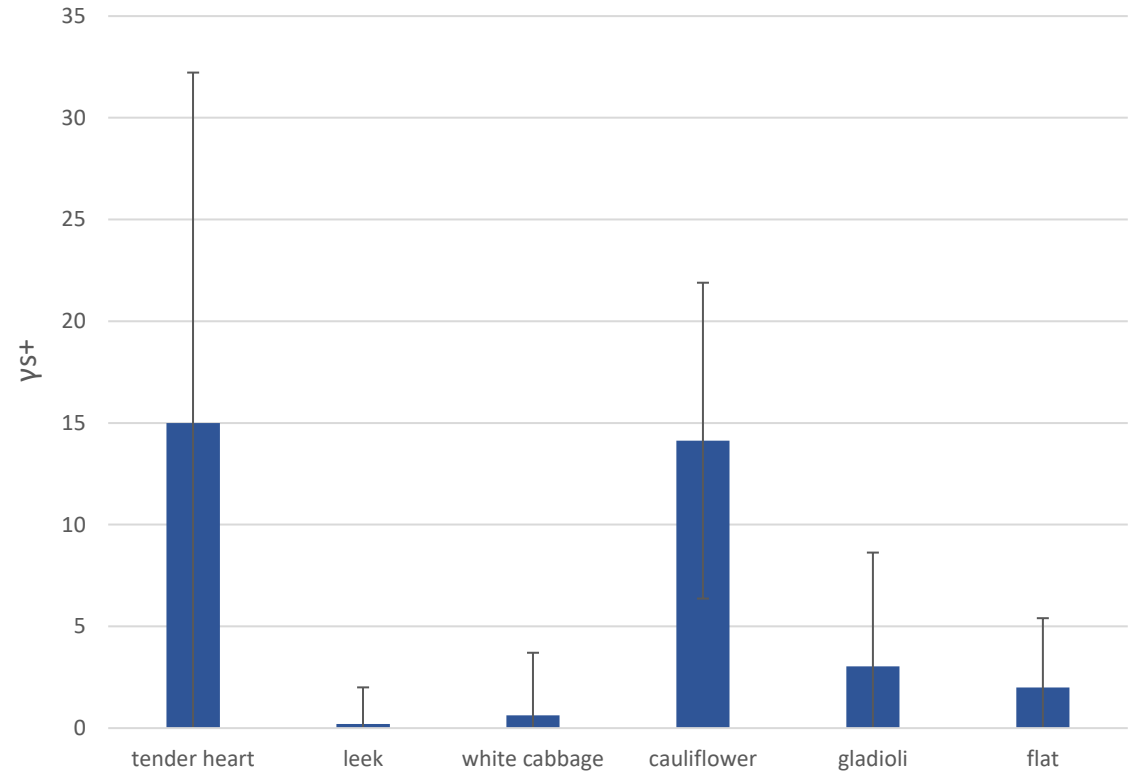


*1e)* Electron acceptor

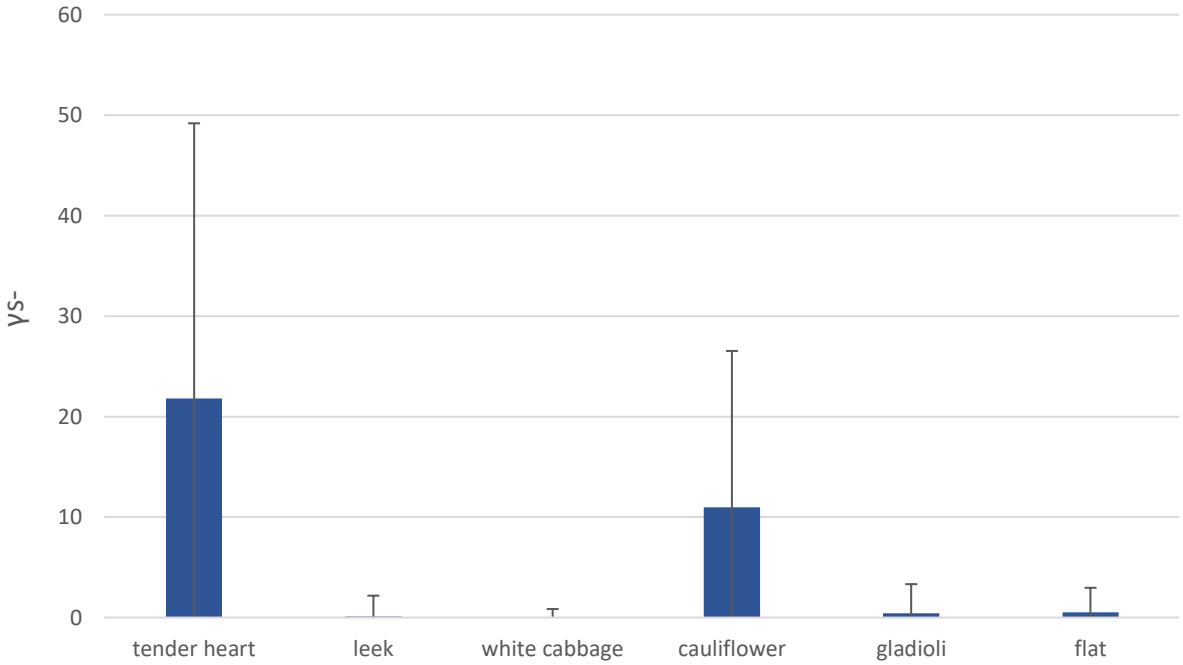


*1f)* Electron donor

Figure 1 Surface energies of the prepared surfaces

## Surface Topographies

The topography of the surfaces was analysed to determine roughness values.

### *Arithmetical mean deviation of the surface roughness ($S_a$)*

When comparing surface $S_a$ several comparisons were statistically significant. When compared to the Tender heart (2.1 µm) surface the Cauliflower (3.4 µm) (P=0.000), Gladioli (2.6µm) (P=0.020), Flat (0.6 µm) (P=0.000) surfaces all showed a significant difference. When compared to the Leek surface the Leek (1.6 µm) surface the Cauliflower (P=0.000), Gladioli (P=0.033), White cabbage (3.8 µm) (P=0.021), and Flat (P=0.000) surfaces all showed a significant difference. When compared to the Cauliflower surface the Gladioli (P=0.021), White cabbage (P=0.000) and Flat (P=0.000) surfaces all showed a significant difference. When compared to the Gladioli surface the White cabbage (P=0.001), and flat (P=0.000) surfaces showed a significant difference. When compared to the White cabbage surface the flat (P=0.000) showed a significant difference. White cabbage, Cauliflower and Gladioli presented with high Sa values. The Flat surface displayed the lowest Sa. In summary, the White cabbage surface was found to have the highest Sa value and the Flat surface showed the lowest (Figure 2a).

### *Root-mean-square deviation of surface topography ($S_q$)*

When comparing surface $S_q$ a number of comparisons were significant. When compared to the Tenderheart (2.2µm) surface the Cauliflower (4.3 µm) (P=0.000) surface showed a significant difference. When compared to the Leek (2 µm) surface the Cauliflower (P=0.000), Gladioli (3.9 µm) (P=0.000), White cabbage (5.2 µm) (P=0.044), and Flat (0.8 µm) (P=0.000) surfaces all showed a significant difference. When compared to the Cauliflower surface the Gladioli (P=0.008), White cabbage (P=0.000) and Flat (P=0.000) surfaces all

showed a significant difference. When compared to the Gladioli surface the White cabbage (P=0.001) and Flat (P=0.00) surfaces showed a significant difference. When compared to the White cabbage surface the flat (P=0.00) surface showed a significant difference. In summary, the White cabbage surface presented with the highest Sq values while the Flat surface displayed the lowest. (Figure 2b).

***Mean peak to valley height of surface topography ($S_{pv}$)***

When comparing surface $S_{pv}$ the Tender heart (54.3 µm) surface compared with the Cauliflower (57.8 µm) (P=0.002) and Flat (6.7 µm) (P=0.000) surfaces there were significant differences demonstrated. The Leek (38.1 µm) surface compared with the Cauliflower (P=0.000) and Flat (P=0.000) surfaces also showed significant differences. The Cauliflower surface compared with the White cabbage (52.9 µm) (P=0.014), Gladioli (60.3 µm) (P=0.019) and Flat (P=0.000) surfaces showed significant differences, as well as the White cabbage surface compared with the Flat (P=0.000) surface. In summary, the Gladioli surface was found to have the highest mean peak to valley height of surface topography and the Flat surface had the lowest (Figure 2c).

*a)*

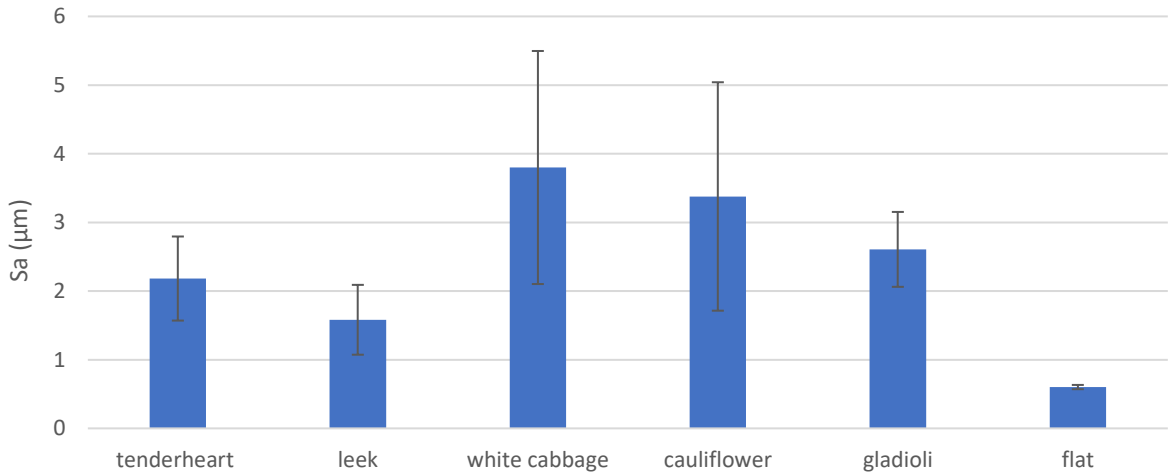

b)

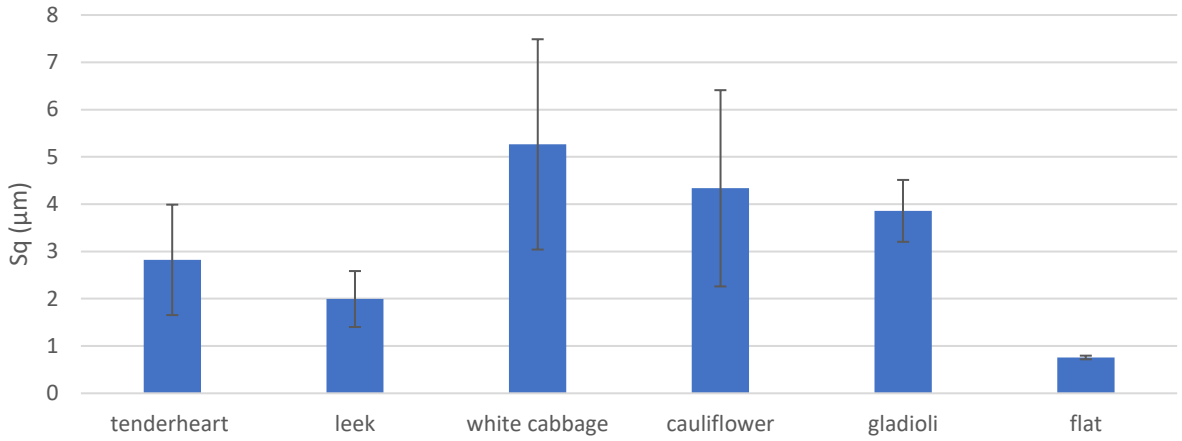


c)

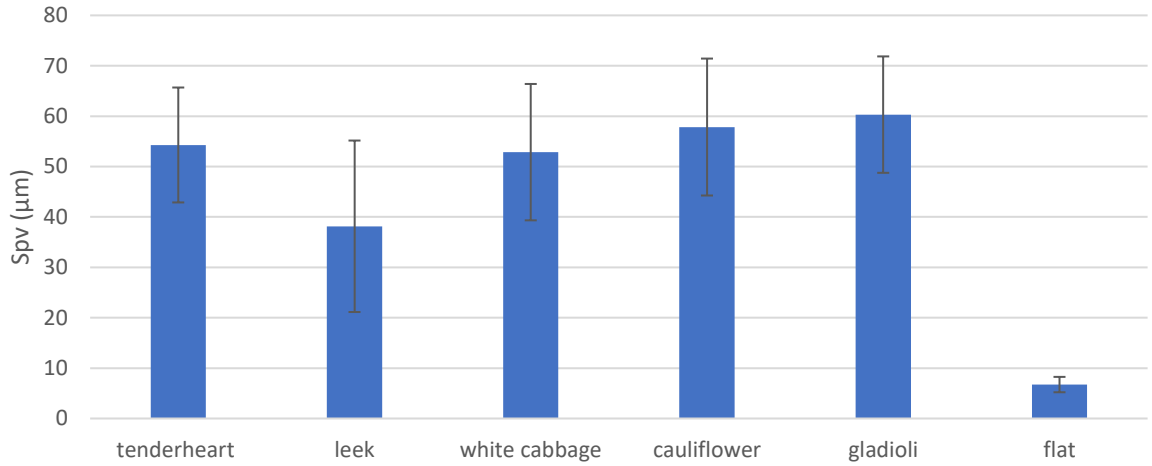


Figure 2 Surface topographies of the prepared surfaces a) Arithmetical mean deviation (Sa) b) Root-mean-square deviation of surface topographies (Sq) c) Mean peak to valley height of surface topographies (Spv)

**Colony-forming units/ mL (CFU/mL) analysis**

Surfaces were analysed with attachment, adhesion and retention assays to determine the effect varying topographies had on pre-biofilm surface colonisation.

***E. coli* in monoculture**

*Attachment assays*

No significant difference was found when comparing the numbers following the bacterial attachment assays. The Leek (6.3 $Log_{10}$ CFU/$cm^2$) surface displayed the highest number of *E. coli* cells attached. The Gladioli (6.2 $Log_{10}$ CFU/$cm^2$) and Flat (6.3 $Log_{10}$ CFU/$cm^2$) surfaces displayed centrally in the range of data. The Cauliflower (6.1 $Log_{10}$ CFU/$cm^2$) surface displayed the lowest number of *E. coli* cells attached, followed by the Tenderheart (4.12 $Log_{10}$ CFU/$cm^2$) and White cabbage (6.12 $Log_{10}$ CFU/$cm^2$) surfaces. In summary, the Cauliflower surface was found to prevent attachment of *E. coli* cells the most and the Leek surface displayed the highest number of cells attached (Figure 3).

*Adhesion assays*

No significant difference was found when comparing the results of the bacterial adhesion experiments of *E. coli* in monoculture. The Leek (6.7 $Log_{10}$ CFU/$cm^2$) surface displayed the highest *E. coli* cells adhered, flowed by the Gladioli (6.6 $Log_{10}$ CFU/$cm^2$) surface. The White cabbage (6.5 $Log_{10}$ CFU/$cm^2$) and Cauliflower (6.57 $Log_{10}$ CFU/$cm^2$) surfaces were found to be central in the range of data. The Flat (6.26 $Log_{10}$ CFU/$cm^2$) surface displayed the lowest number of cells adhered flowed by the Tenderheart (2.3 $Log_{10}$ CFU/$cm^2$) surface. In summary, the Flat surface was found to prevent adhesion of *E. coli* cells the most while the Leek surfaces displayed the highest number of cells adhered (Figure 3).

*Retention assays*

Several significant differences were found when comparing the bacterial retention assays. The Cauliflower (4.4 $Log_{10}$ CFU/$cm^2$) surface compared with the Tenderheart (4.2 $Log_{10}$ CFU/$cm^2$) (P=0.046), Leek (4.6 $Log_{10}$ CFU/$cm^2$) (P=0.046) White cabbage (3.6 $Log_{10}$ CFU/$cm^2$) (p=0.052) and Flat (5.4 $Log_{10}$ CFU/$cm^2$) (P=0.021) surfaces was all found to be significant. No significant difference was found when the Gladioli (4.7 $Log_{10}$ CFU/$cm^2$) surface was compared to all other surfaces. The Flat surface presented with the highest number of *E. coli* cells retained, while the White Cabbage presented with the lowest. In summary, the White cabbage surface was found to prevent retention of *E. coli* cells the most while the Flat surfaces retained the highest number of cells (Figure 3).

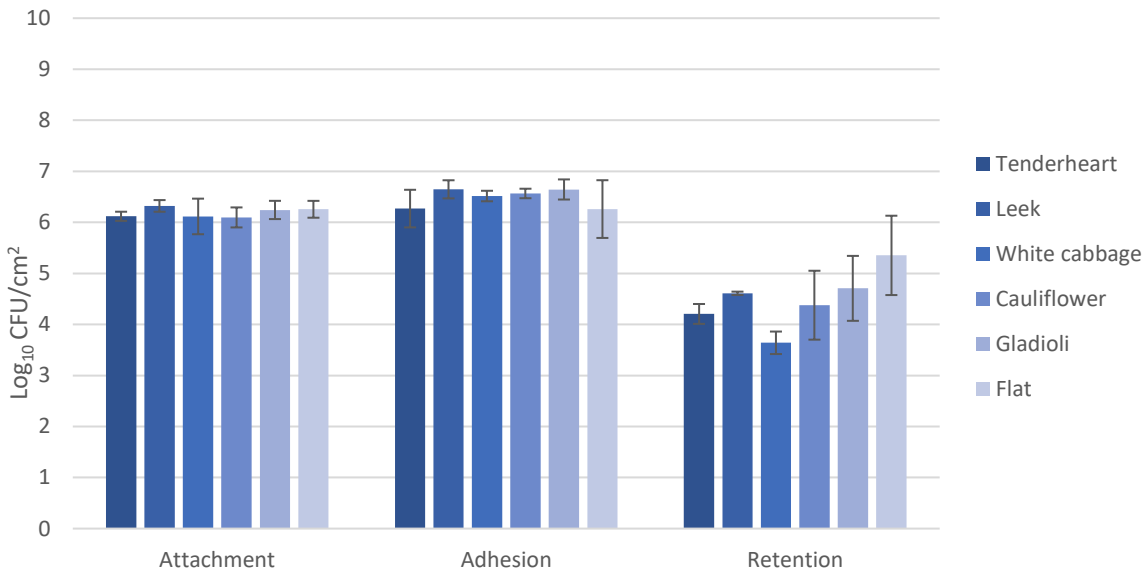


Figure 3 *E. coli* attachment, adhesion and retention of biomimetic surfaces presented as $Log_{10}$ CFU/$cm^2$.

### *L. monocytogenes* in monoculture

*Attachment assays*

When compared to the White cabbage (6.0 $Log_{10}$ CFU/$cm^2$) surface, the Gladioli (6.1 $Log_{10}$ CFU/$cm^2$) (P=0.046) and Tender heart (6.2 $Log_{10}$ CFU/$cm^2$) (P=0.0009) surfaces showed significant differences concerning the numbers of bacteria attached. The Cauliflower (6 $Log_{10}$ CFU/$cm^2$) surface-displayed central in the range of data. In summary, the Leek surface displayed the most *L. monocytogenes* cells attached while the Flat surface showed the least (Figure 4).

*Adhesion assays*

When compared to the White cabbage (6.8 $Log_{10}$ CFU/$cm^2$) surface, the Tender heart (6.3 $Log_{10}$ CFU/$cm^2$) (P=0.004), Leek (6.8 $Log_{10}$ CFU/$cm^2$) (P=0.04), and Flat (6.7 $Log_{10}$ CFU/$cm^2$) (P=0.042) surfaces showed significant differences in the results as did the Gladioli (6 $Log_{10}$ CFU/$cm^2$) surface when compared to the Tender heart surface (P=0.012), in relation to bacteria adhered. In summary, the White cabbage surface displayed the highest number of *L. monocytogenes* cells adhered, while the Gladioli surface displayed the least (Figure 4).

*Retention assays*

No significant difference could be found when comparing cells retained. The Leek (5 $Log_{10}$ CFU/$cm^2$) surface retained the highest number of *L. monocytogenes* cells, followed by the Tenderheart (4.5 $Log_{10}$ CFU/$cm^2$) and Flat (4.5 $Log_{10}$ CFU/$cm^2$) surfaces. The Gladioli (3.7 $Log_{10}$ CFU/$cm^2$) surface displayed the lowest number of retained *L. monocytogenes* cells, followed by the White cabbage (4.1 $Log_{10}$ CFU/$cm^2$) and Cauliflower (4.3 $Log_{10}$ CFU/$cm^2$) surfaces. In summary, the Leek surface displayed the highest number of cells retained while the Gladioli surface displayed the lowest (Figure 4).

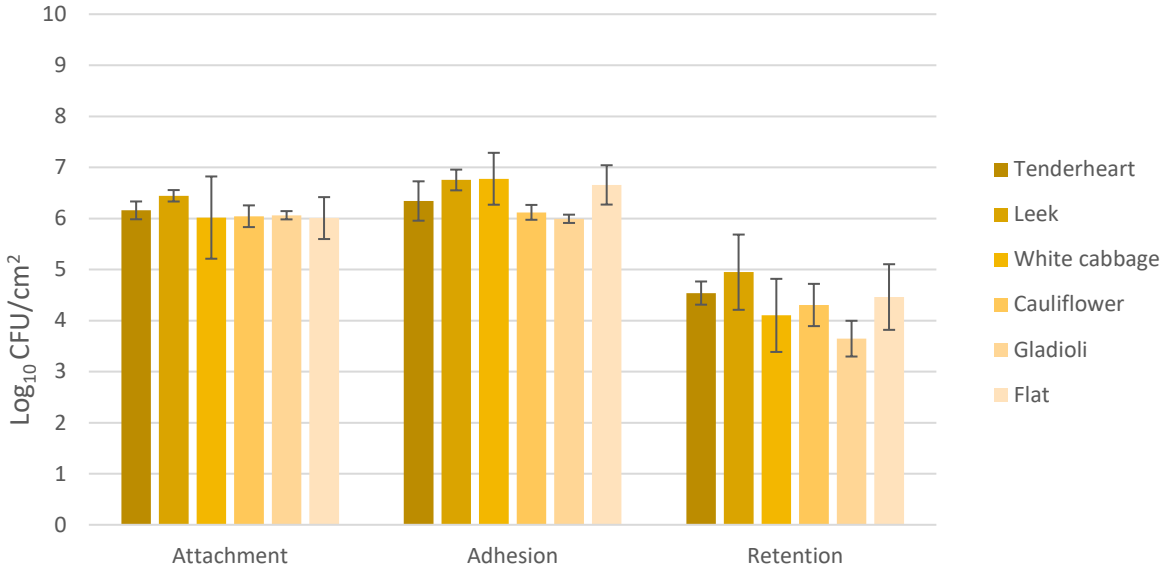


Figure 4 *L. monocytogenes* attachment, adhesion and retention of biomimetic surfaces presented as $Log_{10}$ CFU/$cm^2$.

**Microbial Co-cultures**

Isolation of CFU/cm$^2$ of each species of bacteria was obtained from a 1:1 culture using two varieties of selective growth media.

***E. coli in co-culture***

*E. coli* was isolated from co-culture using MacConkey agar.

*Attachment assays*

The White cabbage (5.5 Log$^{10}$ CFU/cm$^2$) surface was found to be significant when compared to the Tender heart (4.5 Log$^{10}$ CFU/cm$^2$) (P=0.046), Leek (5.1 Log$^{10}$ CFU/cm$^2$) (P=0.046) and Gladioli (6.2 Log$^{10}$ CFU/cm$^2$) (P=0.046) surfaces in relation to *E. coli* cells attached in co-culture. The Gladioli surface displayed the most *E. coli* cells attached followed by the White cabbage and Cauliflower (5.4 Log$^{10}$ CFU/cm$^2$) surfaces. The Tenderheart surface displayed the least amount of *E. coli* cells attached, followed by the Leek and Flat (5.2 Log$^{10}$ CFU/cm$^2$) surfaces. In summary, the Gladioli surface displayed the highest number of cells attached while the Tenderheart surface displayed the lowest (Figure 5).

*Adhesion assays*

When compared to the Leek (6.2 Log$^{10}$ CFU/cm$^2$) surface, the Tender heart (5.1 Log$^{10}$ CFU/cm$^2$) (P=0.049) surface showed a significant difference between the number of cells adhered. The Leek surface displayed the highest number of *E. coli* cells adhered in co-culture, followed by the Gladioli (6.1 Log$_{10}$ CFU/cm$^2$) and Cauliflower (6 Log$_{10}$ CFU/cm$^2$) surfaces. The Tenderheart surface displayed the lowest number of *E. coli* cells adhered in co-culture followed by the White cabbage (5.6 Log$^{10}$ CFU/cm$^2$) and Flat (5.9 Log$^{10}$ CFU/cm$^2$). In summary, the Leek surface displayed the highest number of cells adhered, while the Tenderheart surface showed the least (Figure 5).

*Retention assays*

When compared to the Tender heart (3.4 $Log^{10}$ CFU/$cm^2$) surface, the White cabbage (4.7 $Log^{10}$ CFU/$cm^2$) (P=0.049) and Flat (4.8 $Log^{10}$ CFU/$cm^2$) (P=0.030) surfaces showed a significant difference in the number of cells in relation *to E. coli* retention within the co-culture. Significant differences were also observed when comparing the Cauliflower (4.61 $Log^{10}$ CFU/$cm^2$) surface to the Gladioli (6.18 $Log^{10}$ CFU/$cm^2$) (P=0.033) surface. The Gladioli surface displayed the highest number of *E. coli* cells retained, followed by the Flat and White cabbage surfaces. The Tenderheart surface displayed the lowest number of *E. coli* cells retained, followed by the Leek (5.21 $Log^{10}$ CFU/$cm^2$) and Cauliflower surfaces. In summary, the Gladioli surface displayed the highest number of cells retained while the Tenderheart surface displayed the lowest (Figure 5).

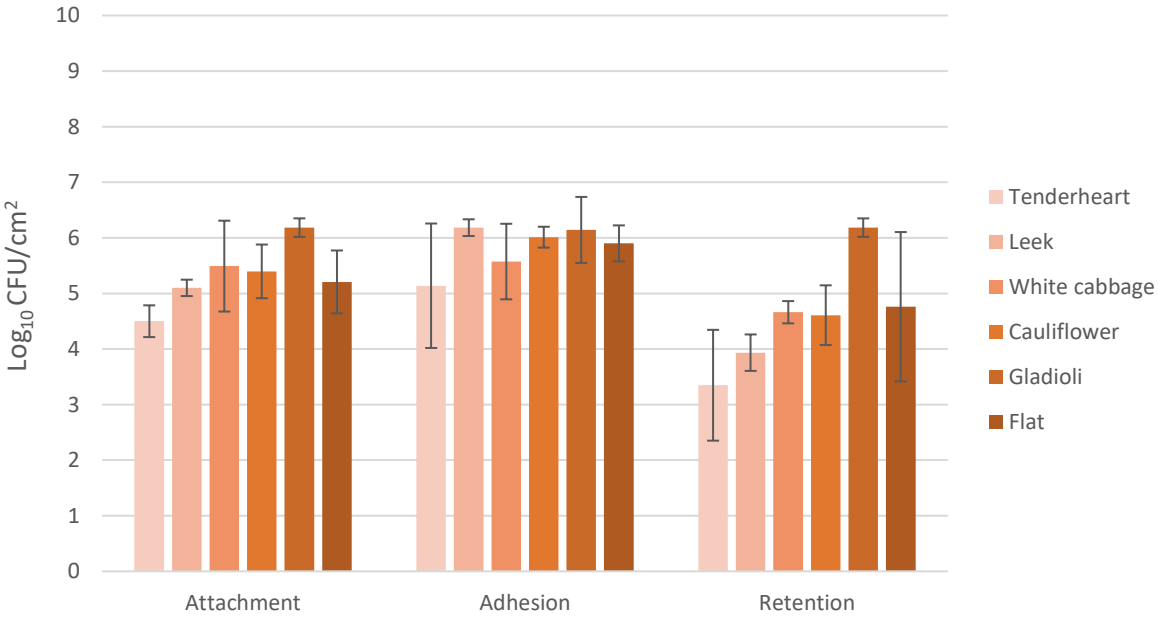


Figure 5 *E. coli* co-culture attachment, adhesion and retention of biomimetic surfaces presented as $Log^{10}$ CFU/$cm^2$.

***L. monocytogenes in co-culture***

*L. monocytogenes* was isolated from co-culture using Oxford growth medium.

*Attachment assays*

In relation to bacterial attachment, White cabbage (6.2 $Log_{10}$ CFU/$cm^2$) showed a significant difference when compared to Tenderheart (5.1 $Log_{10}$ CFU/$cm^2$) (P=0.043) and Gladioli (6.3 $Log_{10}$ CFU/$cm^2$) (P=0.046). The Gladioli surface displayed the highest number of *L. monocytogenes* cells attached, followed by the White cabbage surface. The Tenderheart surface presented with the lowest number of *L. monocytogenes* cells attached followed by the leek (5.5 $Log_{10}$ CFU/$cm^2$), Cauliflower (5.7 $Log_{10}$ CFU/$cm^2$) and Flat (5.8 $Log_{10}$ CFU/$cm^2$) surfaces. In summary, the Gladioli surface displayed the highest number of cells attached while the Tenderheart surface displayed the least (Figure 6).

*Adhesion assays*

No significant difference was found when comparing *L. monocytogenes* cell adhesion in co-culture. The Flat (6.6 $Log_{10}$ CFU/$cm^2$) surface displayed the highest number of *L. monocytogenes* cells adhered, followed by the Leek (6.6 $Log_{10}$ CFU/$cm^2$), Gladioli (6.6 $Log_{10}$ CFU/$cm^2$) and Cauliflower (6.5 $Log_{10}$ CFU/$cm^2$) surfaces. The Tenderheart (6.1 $Log_{10}$ CFU/$cm^2$) surface displayed the lowest number of cells adhered, followed by the White cabbage (6.3 $Log_{10}$ CFU/$cm^2$) surface (Figure 6). In summary, the Flat surface displayed the highest number of cells adhered, while the Tenderheart surface displayed the least.

*Retention assays*

No significant difference could be found when comparing all surfaces concerning bacterial retention with *L. monocytogenes* in co-culture. The Gladioli (5.1 $Log_{10}$ CFU/$cm^2$) surface displayed the highest number of *L. monocytogenes* cells retained, followed by the Flat (4.8

$Log_{10}$ CFU/cm$^2$) and Cauliflower (4.6 $Log_{10}$ CFU/cm$^2$) surfaces. The Tenderheart 3.9 $Log_{10}$ CFU/cm$^2$) surface showed the lowest number of *L. monocytogenes* cells retained, followed by the Leek (4.1 $Log_{10}$ CFU/cm$^2$) and White cabbage (4.3 $Log_{10}$ CFU/cm$^2$) surfaces. In summary, the Gladioli surface displayed the highest number of cells retained, while the Tenderheart surface displayed the least (Figure 6).

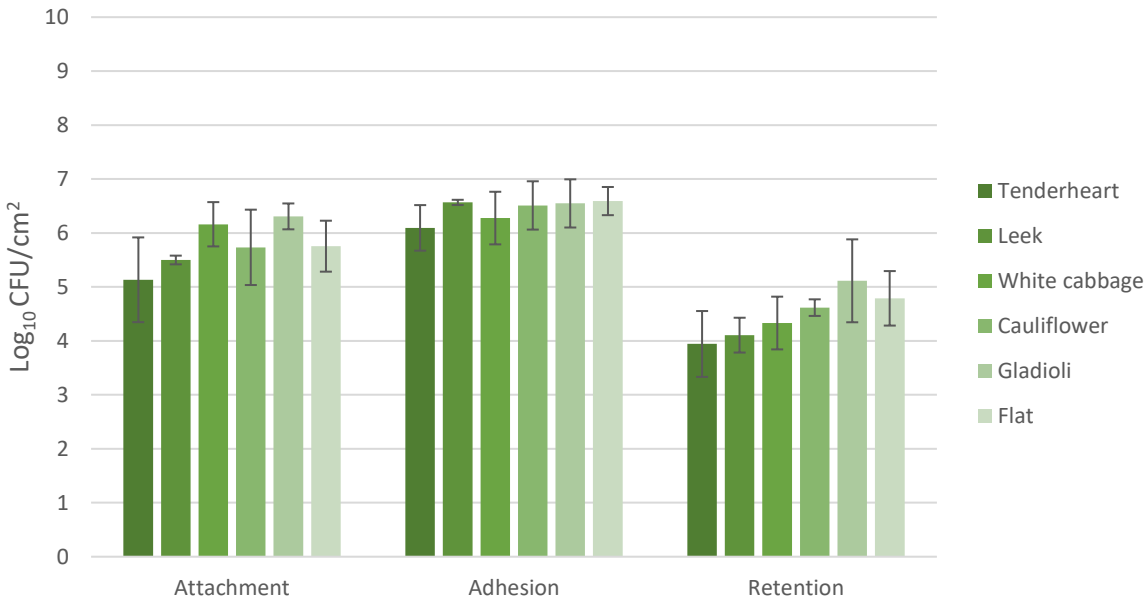


Figure 6 *L. monocytogenes* co-culture attachment, adhesion and retention of biomimetic surfaces presented as $Log_{10}$ CFU/cm$^2$.

**SEM analysis**

Surfaces were analysed with attachment, adhesion and retention assays to determine the effect varying topographies has on pre-biofilm surface colonisation; SEM was used to determine cells /$cm^2$.

***E. coli in monoculture SEM analysis***

*Attachment assays*

None of the results compared in relation to the numbers of bacteria observed following SEM of the bacterial attachment showed a significant difference. The Leek (5.9 $Log_{10}$ cells /$cm^2$) surface presented with the highest number of *E. coli* cells attached, followed by the Tenderheart (5.7 $Log_{10}$ cells /$cm^2$), Gladioli (5.7 $Log_{10}$ cells /$cm^2$) and Flat (5.6 $Log_{10}$ cells /$cm^2$) surface. The White cabbage (4.7 $Log_{10}$ cells /cm2) surface presented with the lowest number of *E. coli* cells attached, followed by the Cauliflower (5.5 $Log_{10}$ cells /$cm^2$) surface. In summary, the Leek surface displayed the highest number of cells attached, while the White cabbage surface displayed the least (Figure 7).

*Adhesion assay*s

None of the results compared in relation to bacterial adhesion showed any significant difference. The Flat (6.3 $Log_{10}$ cells /$cm^2$) surface displayed the highest number of *E. coli* cells adhered, followed by the Gladioli (6.1 $Log_{10}$ cells /$cm^2$), White cabbage (6.0 $Log_{10}$ cells /$cm^2$) and Tenderheart surfaces (5.9 $Log_{10}$ cells /$cm^2$). The Cauliflower (5.4 $Log_{10}$ cells /$cm^2$) surface displayed the least amount of *E .coli* cells adhered closely followed by the Leek (5.7 $Log_{10}$ cells /$cm^2$) surface. In summary, the Flat surface displayed the Highest number of cells (Figure 7).

*Retention assays*

Concerning *E. coli* retention, the comparison of the Tenderheart (4.7 $Log_{10}$ cells /$cm^2$) and Leek (0 $Log_{10}$ cells /$cm^2$) (P=0.000) surfaces was found to be significant. The Cauliflower (4.8 $Log_{10}$ cells /$cm^2$) surface displayed the highest number of *E. coli* cells retained, followed by the White cabbage (4.8 $Log_{10}$ cells /$cm^2$) and Tenderheart surfaces. The Leek surface displayed the lowest number of *E. coli* cells, followed by the Gladioli (4.5 $Log_{10}$ cells /$cm^2$) and Flat (4.5 $Log_{10}$ cells /$cm^2$) surfaces. In summary, the Cauliflower displayed the highest number of cells retained, while the Leek displayed the lowest (Figure 7).

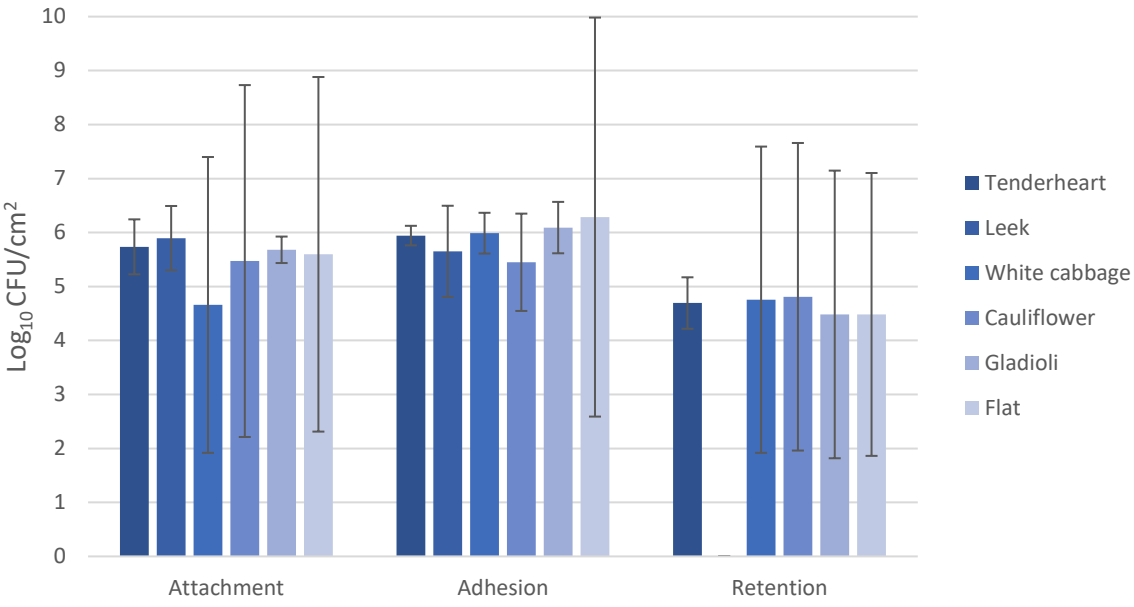


Figure 7 *E. coli* monoculture attachment, adhesion and retention scanning electron enumeration analysis presented as $Log_{10}$ CFU/$cm^2$.

***L. monocytogenes* in monoculture SEM analysis**

*Attachment assays*

A significant difference was found when comparing the Leek (6.1 $Log_{10}$ cells /$cm^2$) and Gladioli (6.8 $Log_{10}$ cells /$cm^2$) surface to the Flat (5.6 $Log_{10}$ cells /$cm^2$) (P=0.029), (P=0.025) surface. The Gladioli surface displayed the highest number of *L. monocytogenes* cells after an attachment assay, followed by the Cauliflower (6.5 $Log_{10}$ cells /$cm^2$), Tenderheart (6.4 $Log_{10}$ cells /$cm^2$) and Leek surfaces. The Flat surface displayed the lowest number of *L. monocytogenes* cells attached, followed by the White cabbage (5.9 $Log_{10}$ cells /$cm^2$) and Leek surfaces. In summary, the Gladioli surface displayed the highest number of cells attached, while the Flat surface displayed the lowest (Figure 8).

*Adhesion assays*

When comparing bacterial adhesion none of the surfaces showed a significant difference in the number of bacteria adhered to the different surfaces. The Gladioli (6.8 $Log_{10}$ cells /$cm^2$) surface displayed the highest number of *L. monocytogenes* cells present after an adhesion assay, followed by the Flat (6.7 $Log_{10}$ cells /$cm^2$), White cabbage (6.7 $Log_{10}$ cells /$cm^2$), Tenderheart (6.6 $Log_{10}$ cells /$cm^2$) and Cauliflower (6.5 $Log_{10}$ cells /$cm^2$) surfaces. The Leek (6.3 $Log_{10}$ cells /$cm^2$) surface presented with the lowest number of *L. monocytogenes* cells present. In summary, the Gladioli surface displayed the highest number of cells adhered, while the Leek surfaces displayed the lowest (Figure 8).

*Retention assays*

A significant difference was found when comparing the numbers of bacteria retained on the Tenderheart (5.9 $Log_{10}$ cells /$cm^2$) surface to the White cabbage (5.2 $Log_{10}$ cells /$cm^2$) (P=0.023) surface. The Cauliflower (6.1 $Log_{10}$ cells /$cm^2$) surface displayed the highest number of *L. monocytogenes* cells present after a retention assay, followed by the Tenderheart and Gladioli (5.8 $Log_{10}$ cells /$cm^2$) surfaces. The Flat (4.7 $Log_{10}$ cells /$cm^2$)

surface displayed the lowest number of *L. monocytogenes* cells present after a retention assay, followed by the White cabbage and Leek (5.6 $Log_{10}$ cells /$cm^2$) surfaces. In summary, the Cauliflower surface displayed the highest number of cells retained, while the Flat surface displayed the lowest (Figure 8).

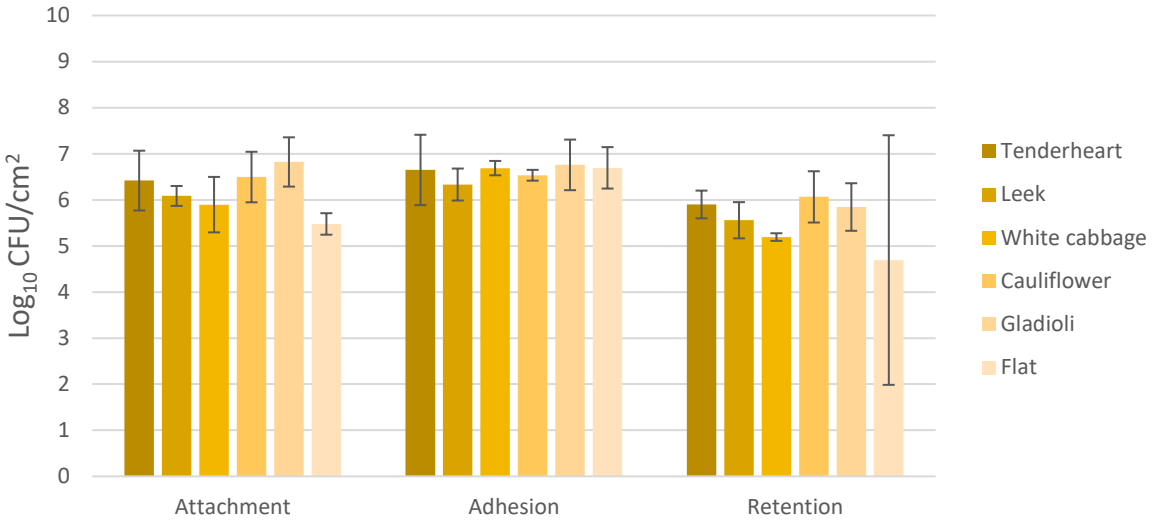


Figure 8 *L. monocytogenes* monoculture attachment, adhesion and retention scanning electron enumeration analysis presented as $Log_{10}$ CFU/$cm^2$.

***E. coli and L. monocytogenes co-culture SEM analysis***

*Attachment assays*

A significant difference was found when comparing the White cabbage (4.1 $Log_{10}$ cells /$cm^2$) surface to the Gladioli (6 $Log_{10}$ cells /$cm^2$) (P=0.046) and Flat (4.9 $Log_{10}$ cells /$cm^2$) (P=0.046) surfaces. The Cauliflower surface displayed the highest number of bacterial cells attached, followed by the Gladioli, Tenderheart (5.6 $Log_{10}$ cells /$cm^2$) and Flat surfaces. The White cabbage surface displayed the lowest number of bacterial cells attached followed by the Leek (4.6 $Log_{10}$ cells /$cm^2$) surface. In summary, the Cauliflower surface displayed the highest number of cells attached, while the White cabbage surface displayed the lowest (Figure 9).

*Adhesion assays*

No significant difference could be found when comparing bacterial adhesion of the co-cultures. The Tenderheart (6.6 $Log_{10}$ cells /$cm^2$) surface displayed the highest number of bacterial cells adhered followed by the Leek (6.3 $Log_{10}$ cells /$cm^2$), Flat (6.2 $Log_{10}$ cells /$cm^2$) surface. The White cabbage (4.5 $Log_{10}$ cells /$cm^2$) surface displayed the lowest number of bacterial cells, followed by the Cauliflower (5.6 $Log_{10}$ cells /$cm^2$) and Gladioli (5.6 $Log_{10}$ cells /$cm^2$) surfaces. In summary, the Tenderheart surface displayed the highest number of cells adhered, while the White cabbage surface displayed the lowest (figure 9).

*Retention assays*

No significant difference was found when comparing surfaces after the bacterial retention assays. The Flat (4.9 $Log_{10}$ cells /$cm^2$) surface displayed the highest number of bacterial cells retained. Followed by the Gladioli (4.5 $Log_{10}$ cells /$cm^2$) surface. The White cabbage (0 $Log_{10}$ cells /$cm^2$) surface displayed the lowest number of bacterial cells retained, followed by the Tenderheart (4.1 $Log_{10}$ cells /$cm^2$), Leek (4.2 $Log_{10}$ cells /$cm^2$) and Cauliflower (4.2

$Log_{10}$ cells /$cm^2$) surfaces (Figure 9). In summary, the Flat surface displayed the highest number of cells retained, while the White cabbage displayed the lowest (Figure 9).

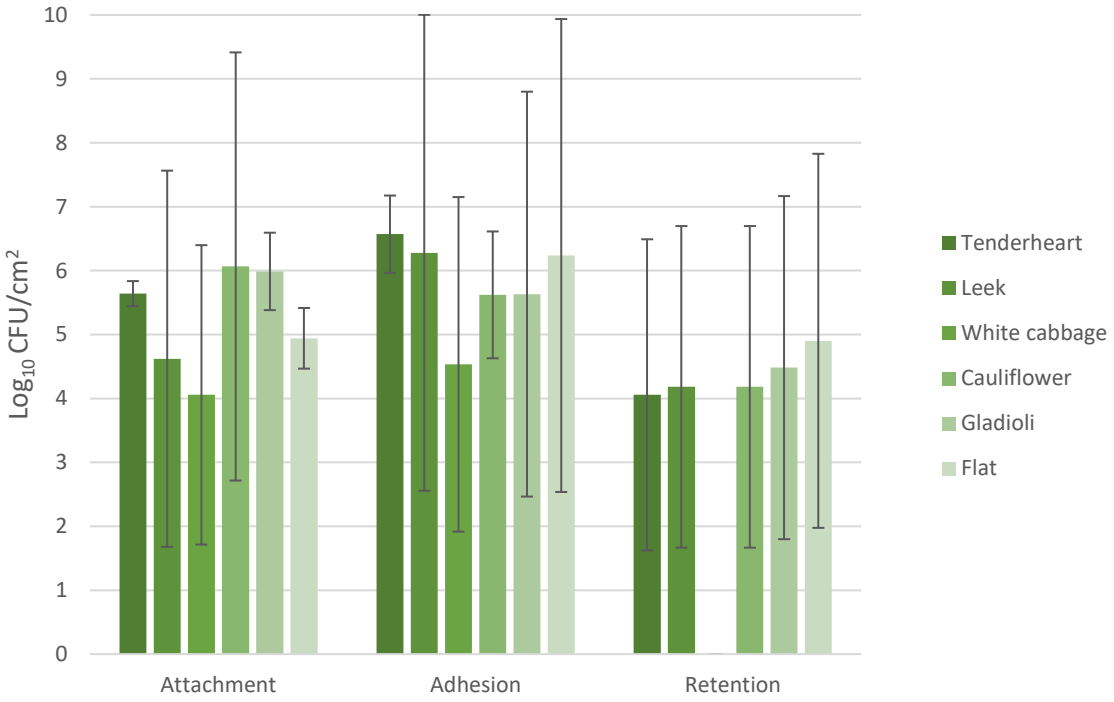


Figure 9 *E. coli* and *L. monocytogenes* monoculture attachment, adhesion and retention scanning electron enumeration analysis presented as $Log_{10}$ CFU/$cm^2$.

## SEM images

### *E. coli in monoculture SEM images*

*Attachment assays*

After an attachment assay on the Tenderheart surface, *E. coli* cells appeared in small shallow surface recesses (~2 μm). No cell clumping was observed (Figure 10a). On the Leek surface following an attachment assay, *E. coli* cells appeared clumped in relatively large groups in large surface recesses. Small groups of cells were also observed on smaller negative surface features (Figure10d). On the Cauliflower surface ensuing an attachment assay, cells were found to be mostly spaced arbitrarily on the surface; however, a small group of cells was observed in a shallow negative surface feature (Figure 10g). Following an attachment assay on the Gladioli surface cells were observed in large shallow ridges along the surface. A small group of cells was observed on top of a large protruding topographical structure (Figure 10j). On the White cabbage surface after an attachment assay, no cells were observed in the image (Figure m). On the Flat surface ensuing an attachment assay, no cells were observed in the image (Figure 10p).

*Adhesion assays*

On the Tenderheart surface after an adhesion assay, cells appeared to be grouped in small clumps predominantly on lower sections of the topography, however, a small clump of cells was also observed in a more elevated and exposed area of the topography (Figure 10b). Following an adhesion assay on the Leek surface, a small clump of cells was observed on the surface with no apparent connection to topography (Figure 10e). On the Cauliflower surface, after an adhesion assay cells appear to be placed on the sides of ridge structures on the surface, small clumping was observed (Figure 10h).

Ensuing an adhesion assay on the Gladioli surface, cells were observed in small clumps on the side of large protruding surface features, with small clumps of cells in large deep surface structures (Figure 10k). Following an adhesion assay on the White cabbage surface, cells appeared to show a clear affinity for deep surface features, with large clumps of cells present in them throughout. Small clumps of cells were also observed on the more exposed areas of the surface (Figure 10n). After an adhesion assay on the Flat surface, cells were observed in sheltered areas of the surface, with these areas presenting with the largest clumps present on the surface, however, an even coating of cells can be seen throughout the image (Figure 10q).

*Retention assays*

Following a retention assay on the Tenderheart surface, only one independent cell was observed on the surface, no large surface features were observed (Figure 10c). After a retention assay on the Leek, cauliflower and gladioli surfaces no cells were observed in the image (Figure 10f,i,l). Ensuing a retention assay on the White cabbage surface, two independent cells were observed in a large shallow negative surface feature (Figure 10o). ). Following a retention assay on the Gladioli surface, no cells were observed in the image (Figure 10r).

In summary, an increased frequency of cells clumping was observed when cells were within proximity to larger negative and positive surface features like those present on the Gladioli and White cabbage surfaces. Smoother surfaces like the Flat surface showed cells predominately independent from one another. Surfaces analysed after attachment and adhesion assays generally displayed more cell clumping than surfaces after a retention assay (Figure 10).

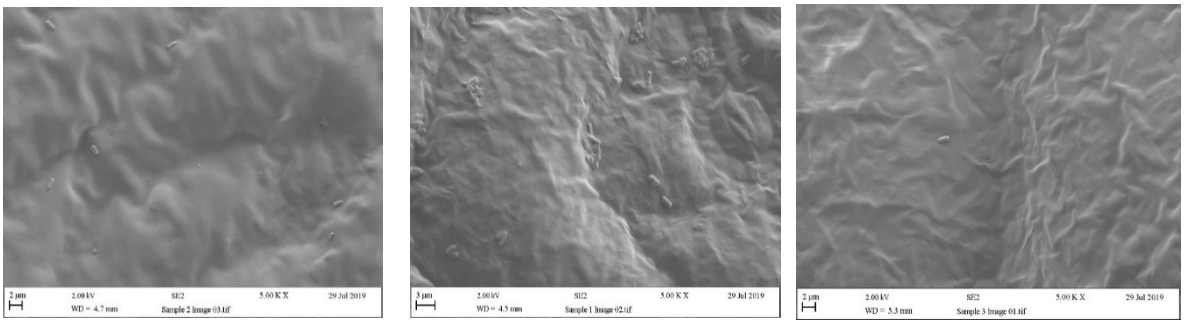

a) b) c)

Figure 10 SEM *E. coli* Tenderheart attachment (a), adhesion (b) and retention (c)

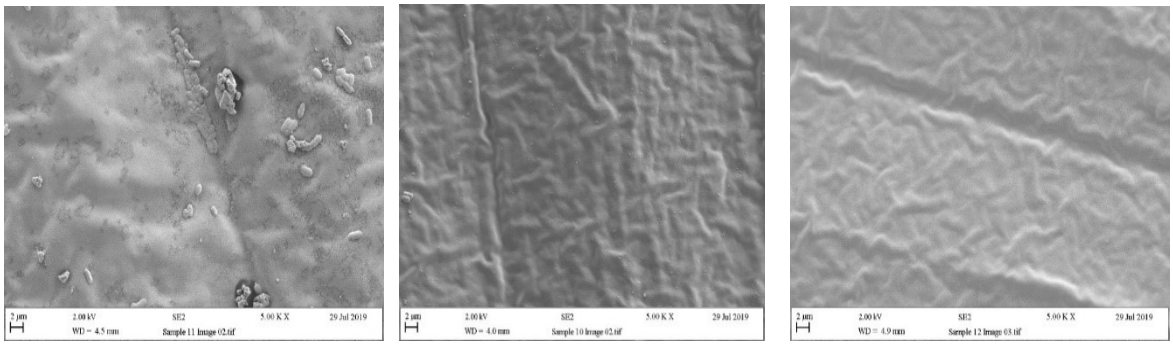

a) b) c)

Figure 11 SEM *E. coli* Leek attachment (a), adhesion (b) and retention (c)

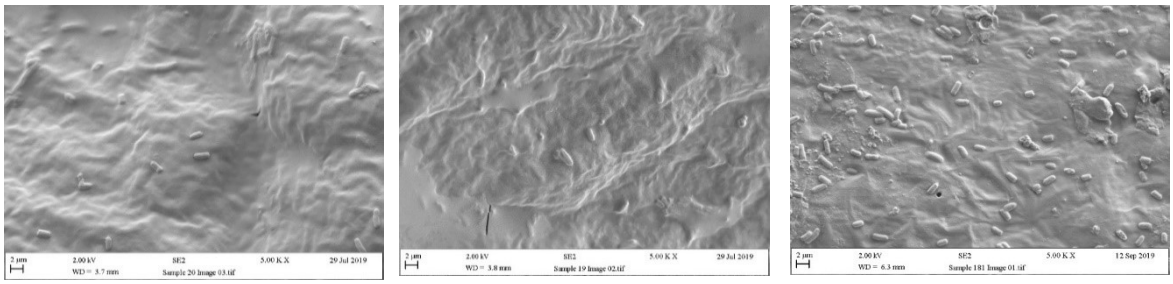

a) b) c)

Figure 12 SEM *E. coli* Cauliflower attachment (a), adhesion (b) and retention (c)

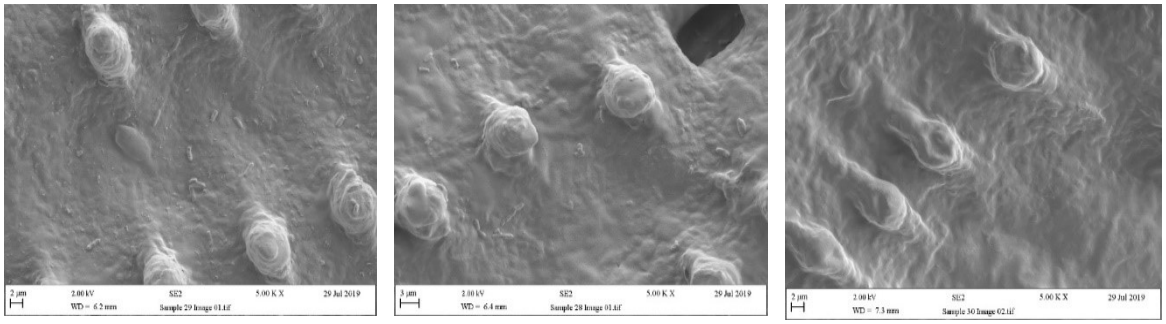

a) b) c)

Figure 13 SEM *E. coli* Gladioli attachment (a), adhesion (b) and retention (c)

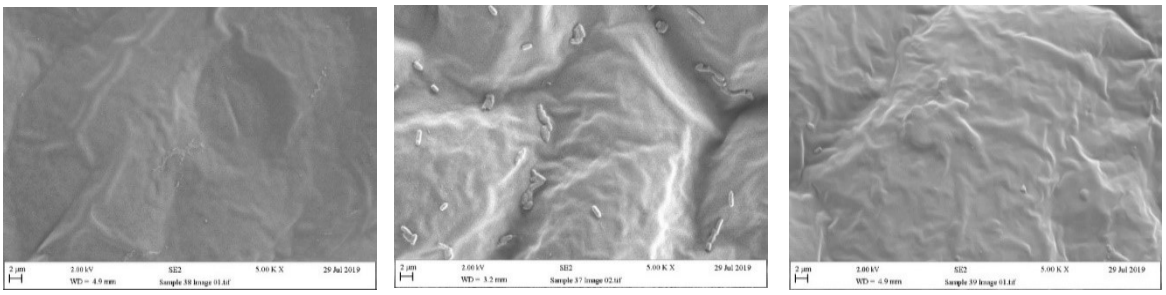

a) b) c)

Figure 14 SEM *E. coli* White cabbage attachment (a), adhesion (b) and retention (c)

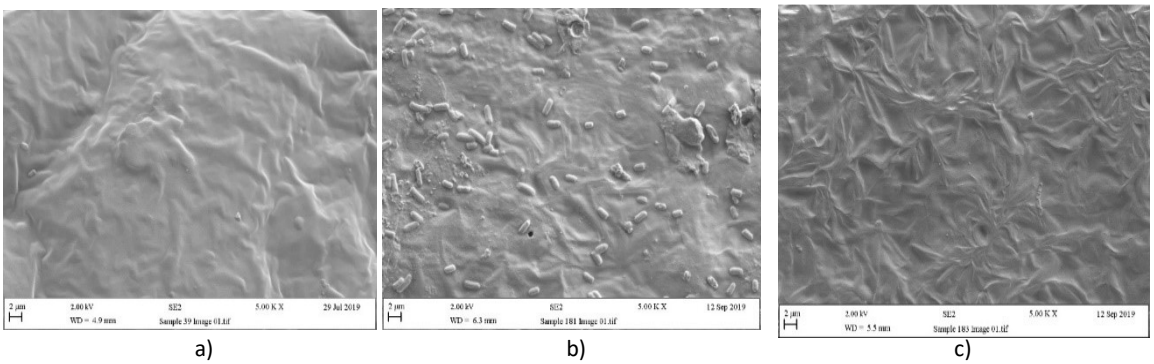

a) b) c)

Figure 15 SEM *E. coli* Flat attachment (a), adhesion (b) and retention (c)

### *L. monocytogenes in monoculture SEM images*

*Attachment assays*

After an attachment assay on the Tenderheart surface cells were observed clumped in multiple sheltered areas on the surface, with no cells present on more exposed areas (Figure 11a). Following an attachment assay on the Leek surface cells were observed to be arbitrarily spaces on the surface with surface topography having little to no visible influence (Figure 11d). Ensuing an attachment assay on the Cauliflower surface cells were found to be arranged in numerous large clumps on the side of surface ridges, with little cells in the lower grooves beneath (Figure 11g). After an attachment assay on the Gladioli surface cells were observed in large clumps showing an affinity for large positive topographical features, with fewer cells present on lower and smooth areas in the image (Figure 11j). Following an attachment assay on the White cabbage surface cell clumps were observed with a slight affinity shown for areas with a more varied microtopography (Figure 11m). Ensuing an attachment assay on the Flat surface very few cells were observed in the image, no large surface features were observed (Figure 11p).

*Adhesion assays*

After an adhesion assay on the Tenderheart surface, a large clump of cells was observed in a large negative topographical feature. A smaller clump of cells was seen on a less prominent feature. Little to no cells were observed in more exposed areas in the image (Figure 11b). Following an adhesion assay on the Leek surface cell clumping was observed throughout the image with cells showing little to no affinity for surface structures (Figure 11e). Ensuing an adhesion assay on the Cauliflower surface minimal cell clumping was observed, with cells showing an affinity to adhere to lower regions of the large surface feature present in the image (Figure 11h). After an adhesion assay on the Gladioli surface,

small amounts of cell clumping was observed in small microtopography features and areas within proximity to larger surface features (Figure 11k). Following an adhesion assay on the White cabbage surface, cell clumping was observed, and cells appear arbitrarily spaced on the relatively smooth surface (Figure 11n). Ensuing an adhesion assay on the Flat surface large amounts of independent cells were observed with minimal clumping, no large surface features were observed (Figure 11q).

*Retention assays*

After a retention assay on the Tenderheart surface, multiple independent cells were observed in the image, with some showing an affinity for sheltered grooves to which the cells are aligned to fit within (Figure 11c). Following a retention assay on the Leek surface, multiple independent cells were observed with some aligned in surface grooves and some retained on the side of surface structures (Figure 11f). Ensuing a retention assay on the Cauliflower surface, large clumps of cells were observed in the more sheltered areas in the image, some independent cells were observed also (Figure 11i). After a retention assay on the Gladioli surface, large amounts of cell clumping was observed on the lateral faces of multiple surface features, with some small clumps of cells present on the flatter areas of the image and on the peaks of the large surface structures (Figure 11l). Following a retention assay on the white cabbage surface, small amounts of arbitrarily spaced independent cells were observed on the surface with no cell clumps present (Figure 11o). Ensuing a retention assay on the Flat surface, only one cell was observed in the image, no large surface features were observed (Figure 11r).

In summary, an increased frequency of cells clumping was observed when cells were within proximity to larger negative and positive surface features like those present on the Gladioli

and White cabbage surfaces. Smoother surfaces like the Flat surface showed cells predominately independent from one another. Surfaces analysed after attachment and adhesion assays generally displayed more cell clumping than surfaces after a retention assay (Figure 11).

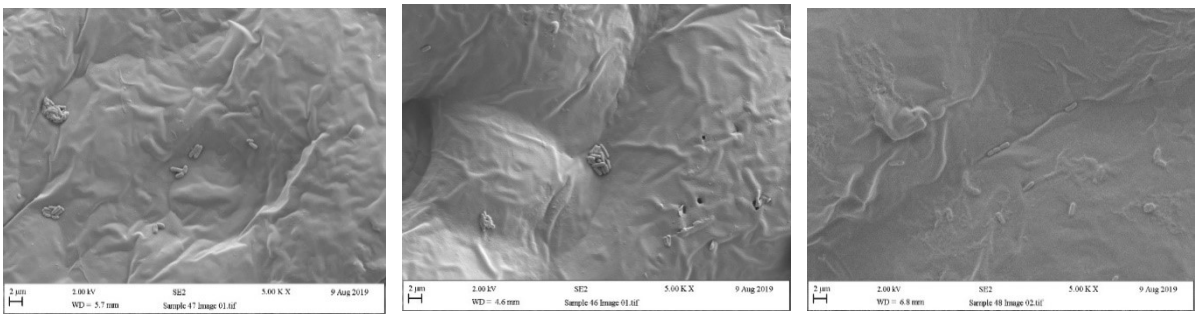

a) b) c)

Figure 16 SEM *L.monocytogenes* Tenderheart attachment (a), adhesion (b) and retention (c)

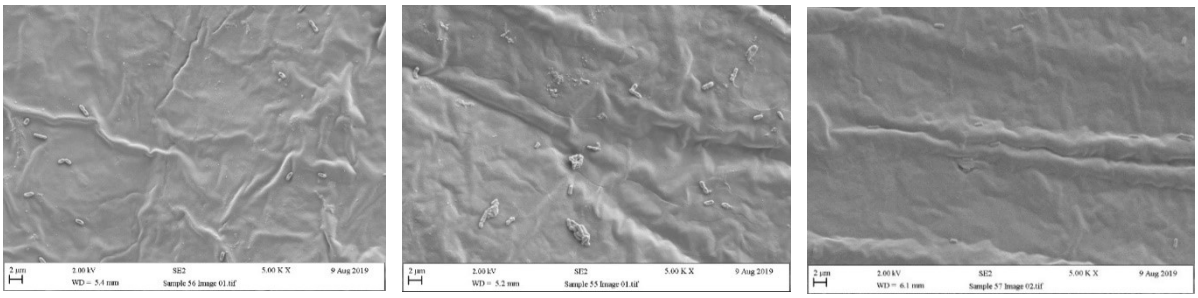

a) b) c)

Figure 17 SEM *L.monocytogenes* Leek (a), adhesion (b) and retention (c)

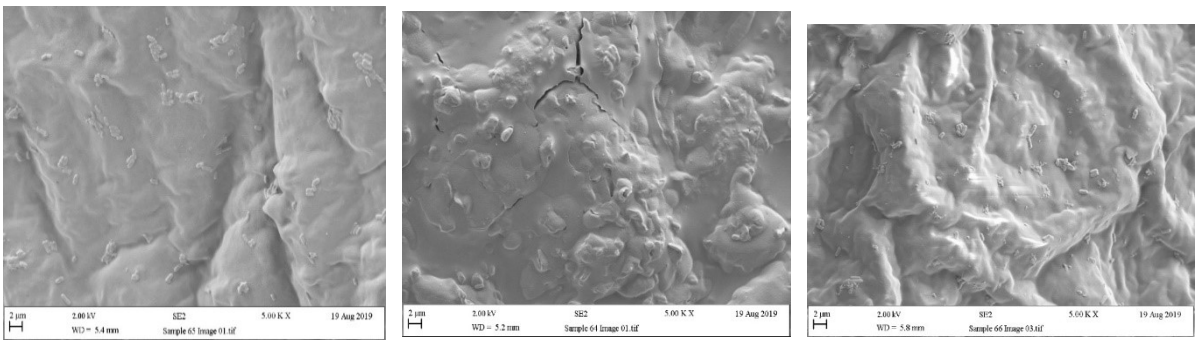

a) b) c)

Figure 18 SEM *L.monocytogenes* Cauliflower attachment (a), adhesion (b) and retention (c)

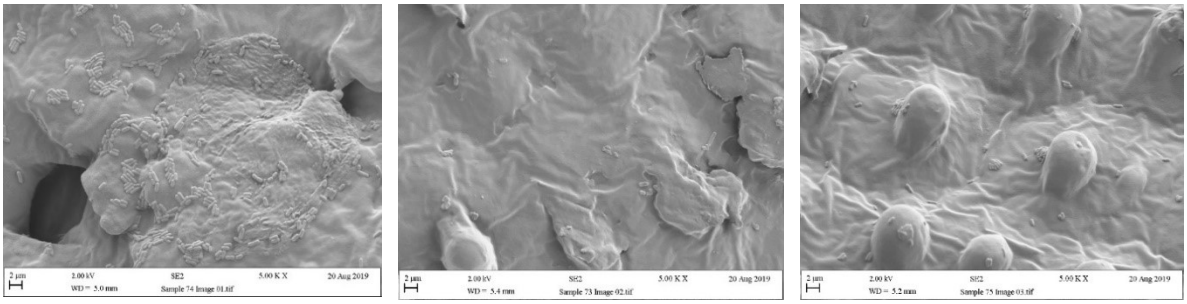

a) b) c)

Figure 19 SEM *L.monocytogenes* Gladioli attachment (a), adhesion (b) and retention (c)

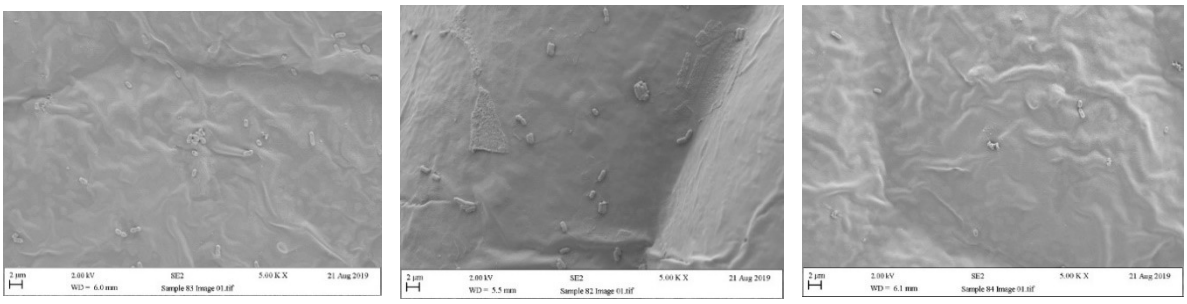

a) b) c)

Figure 20 SEM *L.monocytogenes* White cabbage attachment (a), adhesion (b) and retention (c)

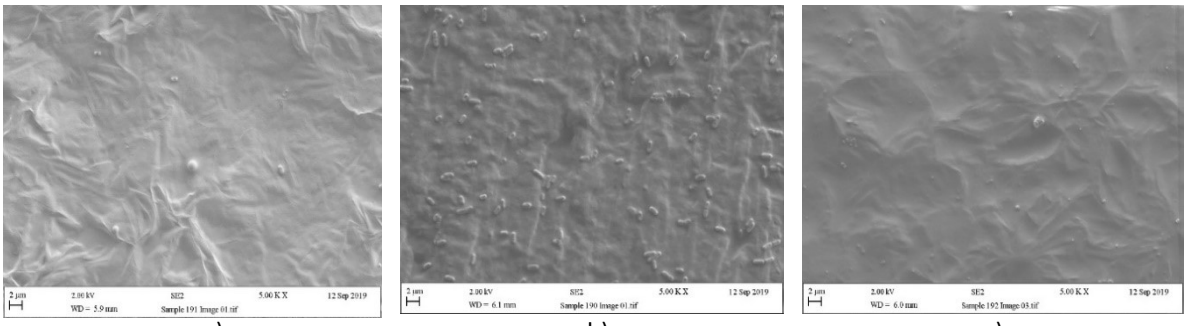

a) b) c)

Figure 21 SEM *L.monocytogenes* Flat (a), adhesion (b) and retention (c)

### *E. coli and L. monocytogenes co-culture SEM images*

*Attachment assay*

After an attachment assay on the Tenderheart surface, cells were observed in small clumps arbitrarily spaced throughout the image; no large clumps of cells were observed (Figure 12a). Following an attachment assay on the Leek surface, no cells were observed in the image (Figure 12d). Ensuing an attachment assay on the Cauliflower surface cells were observed to be independent and showed an affinity of more exposed rougher areas of the topography (Figure 12g). After an attachment assay on the Gladioli surface clumps of cells were observed at the base of large surface features, with independent cells present in the flatter space in-between (Figure 12j). Following attachment assays on the White cabbage and Flat surfaces, no cells were observed in the image (Figure 12m,p).

*Adhesion assays*

After an adhesion assay on the Tenderheart surface, a high frequency of cells in small clumps was observed, with an affinity for more sheltered areas (Figure 12b). Following an adhesion assay on the Leek surface cells were observed to be independent of one another and arbitrarily spaced throughout the image (Figure 12e). Ensuing an adhesion assay on the Cauliflower surface, no cells were observed in the image (Figure 12h). After an adhesion assay on the Gladioli surface, only one cell was observed in the image, however, it was observed to be within the proximity of a large surface structure (figure 12k). Following an adhesion assay on the White cabbage surface, only one cell was observed in the image, however, it was observed to be in the deepest surface groove in the image (Figure12n). Ensuing an adhesion assay on the Flat surface, a large clump of cells was observed in the centre of the image, with large amounts of independent cells throughout. The Large clump appeared to be situated in a shallow negative surface feature (Figure 12q).

*Retention assays*

After a retention assay on the Tenderheart surface, no cells were observed in the image (Figure 12c). After a retention assay on the Leek surface no cell clumping was observed on the relatively flat surface (Figure 12f). Following retention assays on the Cauliflower, Gladioli, White cabbage and Flat surfaces no cells were observed in the image (Figure 12i,l,o,r).

In summary, an increased frequency of cells clumping was observed when cells were within proximity to larger negative and positive surface features such as those present on the Gladioli and white cabbage surfaces. Surfaces without large features such as the flat surface showed cells predominately independent from one another while having seemingly no impact on cell numbers. Surfaces analysed after attachment and adhesion assays generally displayed more cell clumping than surfaces after a retention assay (Figure 12).

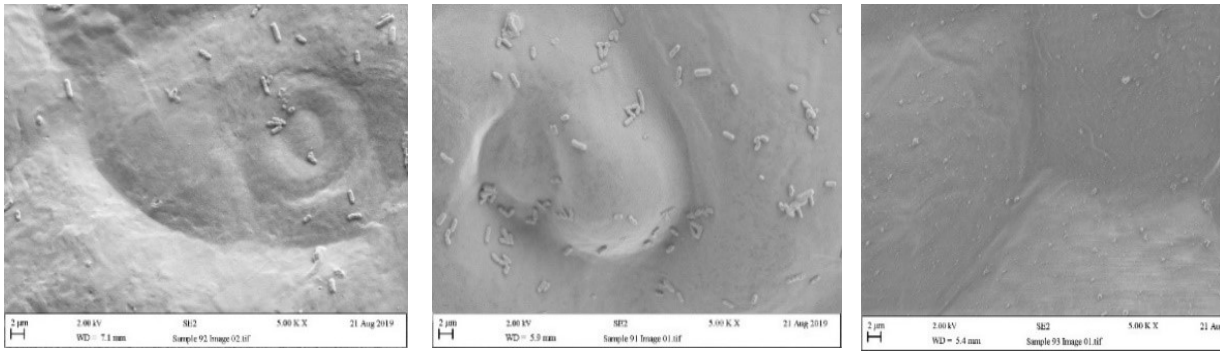

a) b) c)

Figure 22 SEM *E. coli* and *L.monocytogenes* Tenderheart (a), adhesion (b) and retention (c)

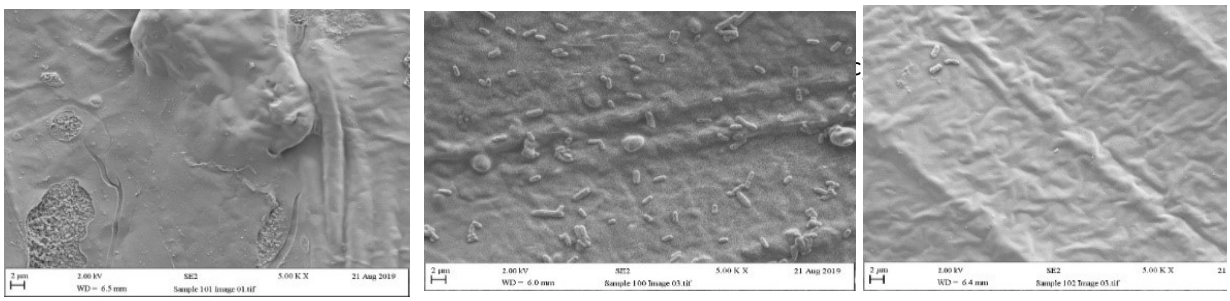

a) b) c)

Figure 23 SEM *E. coli* and *L.monocytogenes* Leek (a), adhesion (b) and retention (c)

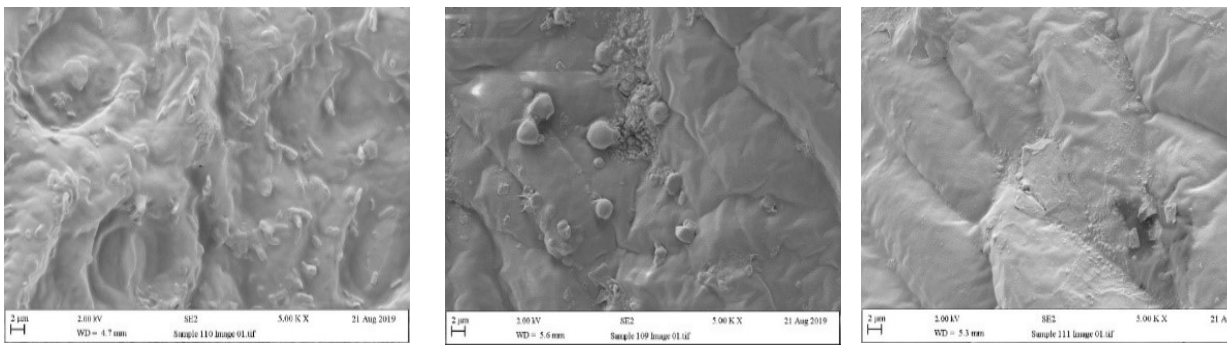

a) b) c)

Figure 24 SEM *E. coli* and *L.monocytogenes* Cauliflower (a), adhesion (b) and retention (c)

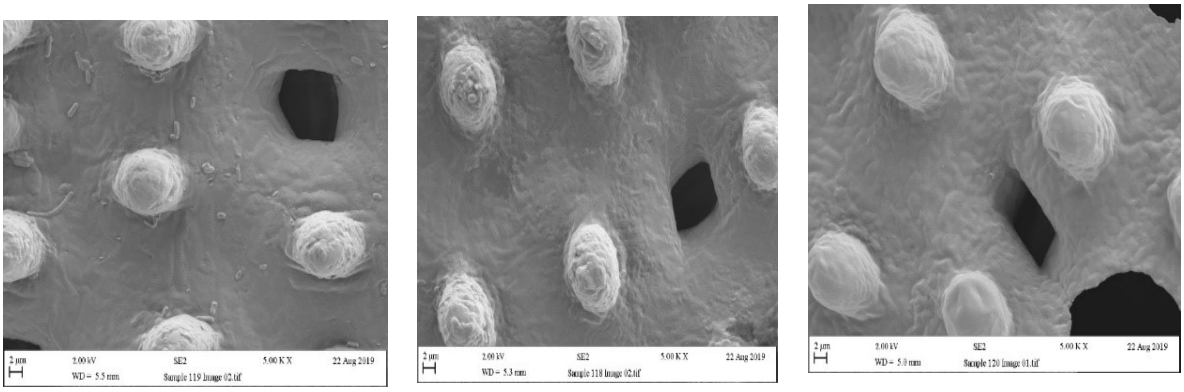

a) b) c)

Figure 25 SEM *E. coli* and *L.monocytogenes* Gladioli (a), adhesion (b) and retention (c)

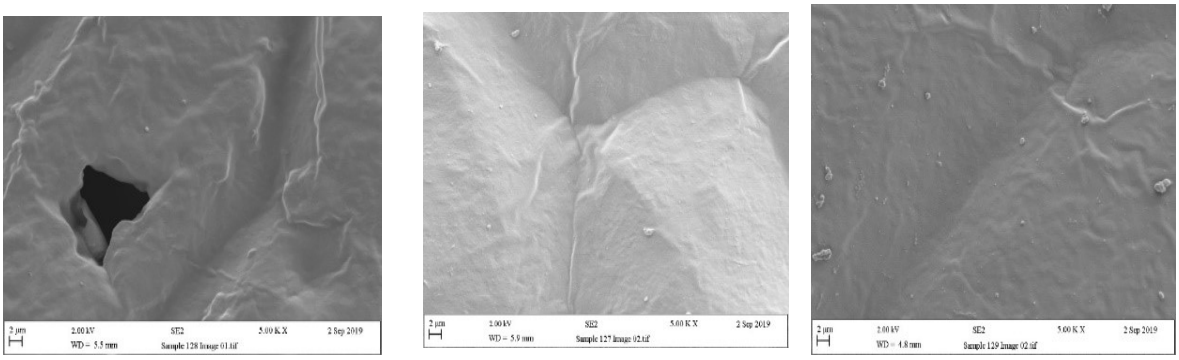

a) b) c)

Figure 26 SEM *E. coli* and *L.monocytogenes* White cabbage (a), adhesion (b) and retention (c)

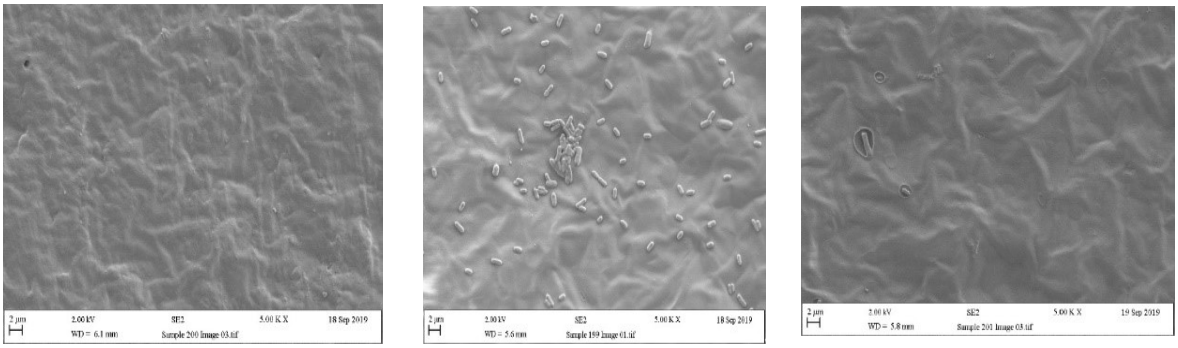

a) b) c)

Figure 27 SEM *E. coli* and *L.monocytogenes* Flat (a), adhesion (b) and retention (c)

## Discussion

Due to the ever-approaching obsolescence of antibiotics and increased consumer attitude towards the environment and use of harsh chemical cleaning products within it, new alternative methods for reducing bacterial fouling in the food industry need to be established. Extensive research has been carried out of surface roughness and physicochemistry and if an ideal combination of factors can be established in relation to bacterial fouling the benefits will far exceed the food industry (Cheng *et al*., 2019; Carniello *et al*., 2018; Wu *et al*., 2018; Song *et al*., 2015). This work looked at different surface characteristics in the form of biomimetic plant leaf surfaces and how their structure and attributes affect the way bacteria begin the process of biofilm development. Bacterial attachment, adhesion and retention were analysed separately to ascertain how each distinct process is influenced by varying surface characteristics.

**Physicochemistry effect on bacteria**

Surface physicochemistry governs surface liquid interactions, dictating how liquids and bacterial cells behave on surfaces. Surface chemistry and topography are the primary influencers of surface physicochemistry (Giovambattista *et al*., 2009). A trend between increased hydrophobicity and reduced levels of bacterial attachment, adhesion and retention of *E. coli* in co-culture after CFU/mL enumeration was established in agreement with (Fadeeva *et al*., 2011) who showed a similar trend. Hydrophobic surfaces have been shown to reduce the contact area of the interface between cell and surface, thus decreasing the adhesion force present (Yuan *et al*., 2017). Gibbs surface free energy (*ΔGiwi*) equates to surface hydrophobicity which is calculated using the Van Oss-Chaudhury-Good equation of the interaction between the surface when immersed in water (Absolom *et al*., 1983).

Free surface energy ($\gamma_s$) when compared to *E. coli* attachment and adhesion in monoculture and *L. monocytogenes* attachment and retention in monoculture exhibited a negative correlation. This is seen in related works (Zhang *et al*., 2015) where a lower difference in surface and bacterial cell $\gamma_s$ resulted in increased levels of bacterial adhesion. The connections between free surface energy and bacterial attachment, adhesion and retention are thought to be a result of interactions between the free surface energy of the bacterial cell, the free surface energy of the surface and the surface tension of the suspending medium (Bollen, 1995). The greater the difference in the surface energy between the surface and bacterial cell, the greater the adhesion force present (Pringle and Fletcher, 1983). A relatively low surface free energy has been shown to be the optimum level for the prevention of bacterial growth on surfaces (Pereni *et al*., 2006). Surface energy is equal to the sum of $\gamma_s^{AB}$ and $\gamma_s^{LW}$ forces, whilst $\gamma_s^{AB}$ is equal to the sum of the $\gamma_s^-$ and $\gamma_s^+$ parameters (Chibowski, 2011). A trend was seen in increased *L. monocytogenes* adhesion co-culture assays after

CFU/mL enumeration that correlated to an increased Lifshitz van der Waals ($\gamma_s^{LW}$). It has been suggested that when non-polar $\gamma_s^{LW}$ forces are increased, bacterial attachment and adhesion will also increase (Carniello *et al*., 2018). The relationship between bacterial surface interaction and $\gamma_s^{LW}$ is dependent on a multitude of factors, such as the chemical and physical properties of the bacteria, surface, and water solutions (Absolom *et al*., 1983).

Polar surface energy is notably important concerning bacterial adhesion. A low $\gamma_s^{AB}$ is thought to correlate to less bacterial adhesion (Yuan *et al*., 2017). $\gamma_s^{AB}$ forces are thought to increase with a decrease of separation to a surface, hydrostatic forces are thought to bridge this gap resulting in $\gamma_s^{AB}$ being one of the primary forces of bacterial adhesion (Mao *et al*., 2011). This was not seen when comparing bacterial attachment, adhesion and retention possible due to bacterial cell $\gamma_s^{AB}$ repelling the surface (Ista and López, 2013). It has been shown that bacterial cells possess an affinity for surfaces with a high Lewis acid value, which is reliant on the ratio of $\gamma_s^+$ and $\gamma_s^-$ resulting in a positive number (Fontaine *et al*., 1996; Lee, 1996). This was seen in only the negatively charged Lewis base surface which presented the lowest values of attachment, adhesion and retention in *E. coli* and *L. monocytogenes* co-culture after CFU/mL enumeration.

Due to the surfaces displaying both $\gamma_s^-$ and $\gamma_s^+$ values all surfaces were observed to be bipolar (Chibowski, 1992). Under typical, conditions bacterial cell walls are electron donors and can be repelled by surfaces that present a high $\gamma_s^-$. If a surface has a $\gamma_s^+$ of approximate to its $\gamma_s^-$ value then only the net difference should be taken as the surface charge (Hamadi *et al*., 2005). The Tender Heart surface presented as the only surface with a negative net charge, which displayed the lowest levels of attachment, adhesion and retention in *E. coli* and *L. monocytogenes* co-culture after CFU/mL enumeration.

**Surface topography**

Surface topography has been suggested to enhance already present physicochemical interactions on the surface (Marmur, 2003). Surfaces with increased roughness can present a contact angle that deviates substantially from that of a smoother surface (M. W. England *et al*., 2016). This deviation can be a result of the surface being homogeneous to wetting, allowing all the surface features to make direct contact with water described with the Wenzel equation (Marmur, 2003). Alternatively, deviation in surface contact angle can be a result of surface heterogeneity, relying on the Cassie–Baxter model which accounts for diminished contact between surface and liquid due to the presence of air bubbles (Marmur, 2003).

**Surface roughness and its effect on bacteria**

Surface roughness is described as the deviation from the average line of the surface (BiolinScientific, 2019). A correlation between a high Arithmetical mean deviation ($S_a$) and low levels of bacterial retention in monoculture after CFU/mL enumeration was established. This is in disagreement with literature, which states that a reduced surface $S_a$ will display a reduced level of bacterial colonisation (Dantas *et al*., 2016). Retention is the first step in the process of biofilm formation that EPS production occurs (Jayathilake *et al*., 2017). However, since surface $S_a$ has been shown to not affect EPS production, this may suggest that external factors could influence the relationship between $S_a$ and bacterial retention throughout all or some of the process, or that EPS production plays less of a role in bacterial retention than previously thought (Pizarro-Cerda and Cossart, 2006; Najafinobar, 2011).

A trend was seen that agrees with other works (Dantas *et al*., 2016). In relation to $S_a$ and *L. monocytogenes* adhesion in monoculture after CFU/mL enumeration, the surface that

presented the highest $S_a$ showed the highest levels of bacterial adhesion, although the surface with the lowest levels of *L. monocytogenes* after an adhesion assay also displayed a high $S_a$ possibly indicating the influence of external factors such as $S_q$, $S_{pv}$ or surface physicochemical properties (Marmur, 2003).

Increased root-mean-square deviation of surface topography ($S_q$) has been shown to decrease bacterial adhesion and inhibit biofilm formation in other works (Singh *et al*., 2011). This was seen when bacterial retention of *E. coli* in monoculture after CFU/mL enumeration and bacterial retention in co-culture after SEM enumeration were compared to $S_q$. Little is known of the direct mechanisms that result in this correlation, it is possible that surface $S_q$ is linked to surface physicochemistry values thus creating this effect (Marmur, 2003).

A negative correlation was seen when comparing a high surface $S_q$ and $S_a$ to $\gamma_s^{AB}$ $\gamma_s^{LW}$, $\gamma_s^+$ and $\gamma_s^-$, this is possibly due to relatively high variations in surface topography distorting physicochemistry results by the trapping of air in micro and nano features on the surface (Marmur, 2003).

A trend was established between a high mean peak to valley height of surface topography ($S_{pv}$) and a high number of bacterial cells present after attachment and retention assays using *E. coli* and *L. monocytogenes* in monoculture. A surface with a high $S_{pv}$ has a higher degree of variation from the $S_a$ mean surface roughness line. This variation could be due to large protruding surface features or large surface depressions, in the case of the Gladioli surface, it was found to likely be both after analysis with SEM. Recent literature has shown that given that concave topography structures are of comparable size to bacterial cells, an increased number of bacterial cells could likely be due protection from shear forces and turbulent flow (Helbig *et al*., 2016). The assays observed in this trend all included a rinse step that was applied resulting high enough levels of shear force to affect bacterial cells on

the surface. The approximate rinse shear force for the attachment assay was 70 kPa (Sharpe, 2011). The approximate rinse shear force for the retention assay was calculated to be 48 kPa ($p_d = 1/2\ \rho\ v^2$). Both are values that far exceed the minimum levels of shear force needed to affect bacterial attachment and retention by a factor of tens of thousands (Nejadnik *et al*., 2008).

**Monoculture and co-culture bacterial assays**

Results taken from monoculture enumerations were highly varied from each other in relation to the surface that displayed the highest and lowest number of bacterial cells present, whereas samples tested with co-culture presented relatively equivalent results when comparing *E. coli* and *L. monocytogenes* cells attached, adhered and retained, indicating that the relationship between the two species may be an influencing factor. This is likely a result of less experimental variation due to samples being taken from the same samples prepared in the same instance. It is thought that *L. monocytogenes* and *E. coli* do not have a significant effect on each other's growth rate while growing in co-culture (Mellefont *et al*., 2008). Results from the co-culture assays after a CFU/mL enumeration appear to be approximately ten times lower than their monoculture counterparts. This showed a cell reduction of five times what was to be expected due to cell counts being halved when grown on selective agar. Indicating a competitive relationship between the two species of bacteria disagreeing with some works (Mellefont *et al*., 2008). It is possible that while interacting with the surfaces stress was added to the bacteria resulting in the loss of an interspecific equilibrium (Khare and Tavazoie, 2015). This is also conferred by the larger gap between

the number of cells recovered and counted via SEM and CFU enumeration after a retention assay, likely due to the amount of time both species were able to interact with one another.

**SEM enumeration**

Cell enumeration results acquired by the analysis of SEM images differ greatly from results obtained via CFU/mL enumeration. Some SEM results directly contradict relevant literature such as bacterial adhesion analysis with co-culture (Yuan *et al*., 2017). This could be due to potential reasons such as, all samples were treated with glutaraldehyde which is used as a fixative before SEM analysis, which has been shown to provide no increased protection from shear force (Kooten *et al*., 1992). This would account for the reduced cell numbers seen throughout the SEM samples due to the method used to wash glutaraldehyde off the surface. Topographies with large surface structure have been shown to protect bacteria from shear force (Nejadnik *et al*., 2008) explaining why a reduction of bacterial cells is not seen as prominently in surfaces with a raised $S_{pv}$**.**

**SEM cell clumping**

Surfaces with less topographical features and lower overall roughness displayed reduced amounts of cell clumping when compared to surfaces with large prominent surface structures. This was only demonstrated for surfaces that had been subject to a rinse step (attachment and retention assays). Surfaces that have not undergone a rinse step showed greater amounts of cell clumping. This is likely explained by the presence of large surface features which shield cells by aiding in the prevention of cell removal via shear force after rinsing (Nejadnik *et al*., 2008). The effect of shear force on bacterial retention was not expected as it is thought that EPS provides a layer of protection from shear force to cells (Park *et al*., 2011). Protection can be conferred from rinsing even in relatively small shallow

surface features. This is likely due to the bacteria becoming flush with the surface topography thus reducing the shear force applied to the cells(Lazzini et al., 2019).

**SEM negative control**

The SEM images that had not been treated bacteria were not visualised since the bacteria were evident on the surface structures, and no advantage would have been gained from analysing these as the value would have been zero since they had been moulded using aseptic processing.

**Conclusions**

The results demonstrated that the Tenderheart leaf surface was the most hydrophobic with the highest surface free energy, highest $\gamma_s^{AB}$, most electron-donating and most electron-accepting surface. The Leek surface demonstrated the lowest surface free energy. The White cabbage surface was the most non-polar surface, with the least $\gamma_s^{AB}$ properties, the least electron-accepting and least electron-donating surface. However, it had the highest $S_a$ and $S_q$ values. The Cauliflower leaf surface was the least hydrophobic and least nonpolar surface whilst the Gladioli surface was found to have the highest $S_{pv}$ values. Finally, the flat surface showed the lowest $S_a$, $S_q$ and $S_{pv}$ values. Following the attachment, adhesion and retention assays, *E. coli* in monoculture did not show any trends between the surface properties and the number of cells retained. However, for *L. monocytogenes* in monoculture, following the attachment and retention assays, the Flat surface showed the least number of cells. Following the adhesion and retention assays, the Gladioli surface (highest $S_{pv}$ values) displayed the lowest numbers of *L. monocytogenes* cells. Use of the bacteria in co-cultures demonstrated that for both the attachment and retention assays, the Tenderheart surface

(most hydrophobic) displayed the lowest number of cells. SEM analysis did not correlate with the CFU/mL assays. However, for all the assays with *L. monocytogenes,* the flat surfaces (lowest roughness) retained the lowest numbers of cells, and for the co-culture, the White cabbage surface (most hydrophilic) displayed the lowest number of cells. These results demonstrate that when more topographically complex surfaces are analysed, the conclusions drawn between the effect of the surface properties on bacterial attachment, adhesion and retention from more uniform surfaces do not apply. Further, the processes of bacterial attachment, adhesion and retention are different and hence differentiation between these classifications needs to be clarified. It was clear that the different methods gave different results and that the use of different bacteria in monoculture and co-culture also affected the microbial assays. Hence, a new approach needs to be taken to understand the cell: surface interactions on complex surfaces.

**Limitations of the study**

Results taken from bacterial cell SEM enumeration were dissimilar to CFU/mL enumeration data. This may have been due to time constraints and only three SEM images were taken of each sample. The use of a handheld goniometer although convenient may have produced contact angle data that was slightly inaccurate. The Wenzel method although simpler does not account for air pockets present underneath the droplet. The application of a desktop goniometer would likely produce more reliable consistent results that would not have to be mapped by hand thus which was often the case thus increasing the chance of human error. The application of the more complex Cassie–Baxter model would also likely give more reliable results.

**Future work**

The work described in this study looks at the relationship between surface roughness and hydrophobicity compared to bacterial attachment, adhesion and retention. No information on cell grouping, density or cell spacing in co-culture was isolated from the results obtained. The application of multifractal analysis could prove invaluable in the understanding of the greater relationship between bacteria surface interactions (Wickens *et al*., 2014). Fractal analysis is a method of surface topography analysis that presumes surface topography is self-similar on all scales and that scale is described by a value termed the fractal dimension. Fractal analysis has the potential to bring together multiple values from varying surface scales into one quantifiable value. This would allow a holistic point of view to be attained and analysed in relation to surface topographical analysis. A multifractal is described as a fractal that cannot operate in one dimension and a continuous spectrum of dimensions are required for the object to exist (Brown and Scholz, 1985; Wickens *et al*., 2014). The combination of fractal analysis and 3D imaging software has the potential to describe cell clumping, dispersion and density data that can explain the relationship between individual topographical features and bacterial surface interactions at every stage of biofilm formation (Dazzo and Yanni, 2017).

To gain a more comprehensive understanding of all steps of biofilm development the last step in this process must be analysed. Once bacterial are retained on a surface cell proliferation occurs resulting in biofilm formation (Whitehead and Verran, 2015). A crystal violet assay would allow the quantification of biofilms on biomimetic surfaces in monoculture and co-culture (Peeters *et al*., 2008). SEM analysis used in conjunction with this assay could give more comprehensive detailed results such as spacing and distribution data (Badha *et al*., 2019). The application of confocal analysis would allow biofilm structure and architecture to be understood providing images that differentiate between cells in co-

culture displaying their intra-biofilm distribution and organisation (Reichhardt and Parsek, 2019).

Conditioning film analysis assays would prove insightful towards a more complete understanding of biofilm surface interactions. In nature biofilms do not form without there first being a conditioning film present, conditioning film composition directly affects how a biofilm will develop on a surface (Whitehead and Verran, 2015). Analysis with Fourier Transform InfraRed (FTIR) microscopy could give a detailed composition of conditioning films which could be used in conjunction with biofilm analysis (Humbert and Quiles, 2011). Cell surface hydrophobicity analysis could give a more complete understanding of surface physicochemistry by displaying the opposing side of interactions described by data obtained with a goniometer. Microbial adhesion to hydrocarbon (MATH) assay would be able to describe this data (Rosenberg, 2006).

Although a general knowledge of the chemical composition of the dental wax is known, a detailed understanding may prove to be highly insightful in relation to any influence chemicals present have on bacterial growth. Analysis with Fourier-transform infrared spectroscopy (FTIR) would provide this insight.

**References**

Absolom, D. R., Lamberti, F. V., Policova, Z., Zingg, W., van Oss, C. J. and Neumann, A. W. (1983) 'Surface thermodynamics of bacterial adhesion.' Appl Environ Microbiol, 46(1), Jul, pp. 90-97.

Badha, V., Moore, R., Heffernan, J., Castaneda, P., McLaren, A. and Overstreet, D. (2019) 'Determination of Tobramycin and Vancomycin Exposure Required to Eradicate Biofilms on Muscle and Bone Tissue.' J Bone Jt Infect, 4(1) 2019/01/01, pp. 1-9.

Bajpai, P. (2015) Pulp and Paper Industry: Microbiological Issues in Papermaking. Oxford: Elsevier.

Bansal, B. and Chen, X. (2006) 'A Critical Review of Milk Fouling in Heat Exchangers.' Comprehensive reviews in food science and food safety, 5(2) pp. 27.33.

Barkai, H., Elabed, S., Sadiki, M., Boutahari, S., Mounyr, B., Omar, E. F. and Koraichi, S. (2016) 'The Effect of Cellulase Treatment Time on the Cedar Wood Surface Physicochemical Properties.' AMERICAN JOURNAL OF ADVANCED SCIENTIFIC RESEARCH, 3(3) pp. 296-304.

Barthlott, W., Mail, M., Bhushan, B. and Koch, K. (2017) 'Plant Surfaces: Structures and Functions for Biomimetic Innovations.' Nanomicro Lett, 9(2) pp. 23

BiolinScientific. (2019) 'Influence of surface roughness on contact angle and wettability. 'Hubspot.net. 7, [Online] [23rd August 2019]

https://cdn2.hubspot.net/hubfs/516902/Pdf/Attension/Tech%20Notes/AT-TN-07-Surface-roughness-CA-wettability.pdf

Bollen, Q. (1995) 'The influence of surface roughness and surface-free energy on supra- and subgingival plaque formation in man.' Journal of Clinical Periodontology, 22 pp. 1-14.

Bonaventura, D., Piccolomini, R., Paludi, D., D'orio, V., Vergara, A., Conter, M. and Ianieri, A. (2008) 'Influence of temperature on biofilm formation by Listeria monocytogenes on various food-contact surfaces: relationship with motility and cell surface hydrophobicity.' Journal of applied microbiology, 104 pp. 1552-1561.

Bos, R., van der Mei, H. C., Gold, J. and Busscher, H. J. (2000) 'Retention of bacteria on a substratum surface with micro-patterned hydrophobicity.' FEMS Microbiol Lett, 189(2), pp. 311-315.

Boyan, B. D., Lotz, E. M. and Schwartz, Z. (2017) 'Roughness and Hydrophilicity as Osteogenic Biomimetic Surface Properties.' Tissue Eng Part A, 23(12), 2017/11/04, pp. 1479-1489.

Brown, S. and Scholz, C. (1985) 'Broad Bandwidth Study of the Topography of Natural Rock Surfaces.' Journal of geophysical research, 90 pp. 12,575-12,582.

Buschhaus, C., Herz, H. and Jetter, R. (2007) 'Chemical composition of the epicuticular and intracuticular wax layers on the adaxial side of Ligustrum vulgare leaves.' New Phytol, 176(2) 2007/08/13, pp. 311-316.

Camargo, A. C., Woodward, J. J., Call, D. R. and Nero, L. A. (2017) 'Listeria monocytogenes in Food-Processing Facilities, Food Contamination, and Human Listeriosis: The Brazilian Scenario.' Foodborne Pathog Dis, 14(11) pp. 623-636.

Carniello, V., Peterson, B. W., van der Mei, H. C. and Busscher, H. J. (2018) 'Physico-chemistry from initial bacterial adhesion to surface-programmed biofilm growth.' Adv Colloid Interface Sci, 261 pp. 1-14.

Centre for disease control (2016) Surveillance for Foodborne Disease Outbreaks, United States, 2016: Annual Report. Atlanta GA: (CDC Report)

Chen, L. H., Köseoğlu, V. K., Güvener, Z. T., Myers-Morales, T., Reed, J. M., D'Orazio, S. E., Miller, K. W. and Gomelsky, M. (2014) 'Cyclic di-GMP-dependent signaling pathways in the pathogenic Firmicute Listeria monocytogenes.' PLoS Pathog, 10(8), DOI: 10.1371/journal.ppat.1004301

Cheng, Y., Feng, G. and Moraru, C. I. (2019) “Micro- and Nanotopography Sensitive Bacterial Attachment Mechanisms: A Review”, p. 191.

Chibowski, E. (1992) 'Solid surface free energy components determination by the thin-layer wicking technique.' Journal of Adhesion Science and Technology, 6(9) pp. 1069-1090.

Chibowski, E. (2011) 'Apparent Surface Free Energy of Superhydrophobic Surfaces.' Journal of Adhesion Science and Technology, 25 pp. 1323-1336.

Colagiorgi, A., Bruini, I., Di Ciccio, P. A., Zanardi, E., Ghidini, S. and Ianieri, A. (2017) 'Listeria monocytogenes Biofilms in the Wonderland of Food Industry.' Pathogens, 6(3) DOI: 10.3390/pathogens6030041

Dantas, L. C., da Silva-Neto, J. P., Dantas, T. S., Naves, L. Z., das Neves, F. D. and da Mota, A. S. (2016) 'Bacterial Adhesion and Surface Roughness for Different Clinical Techniques for Acrylic Polymethyl Methacrylate.' Int J Dent, 2016 DOI: 10.1155/2016/8685796

Dazzo, F. and Yanni, Y. (2017) 'Spatial ecology of microbial colonization intensity and behavior in rice rhizoplane biofilms analyzed by CMEIAS Bioimage Informatics software.' Journal of soil science and plant nutrition, 1(1)

Donlan, R. M. (2002) 'Biofilms: microbial life on surfaces.' Emerg Infect Dis, 8(9) pp. 881-890.

Duta, L., Popescu, A. C., Zgura, I., Preda, N. and Mihailescu, I. N. (2015) 'Wettability of Nanostructured Surfaces.' intechopen, DOI: 10.5772/60808

England, M. W., Sato, T., Yagihashi, M., Hozumi, A., Gorb, S. N. and Gorb, E. V. (2016) 'Surface roughness rather than surface chemistry essentially affects insect adhesion.' Beilstein J Nanotechnol, 7, pp. 1471-1479.

Public Health England (2018) Listeriosis in England and Wales Summary for 2017, London: HSMO. (Goodfellow Report)

Ensikat, H. J., Ditsche-Kuru, P., Neinhuis, C. and Barthlott, W. (2011) 'Superhydrophobicity in perfection: the outstanding properties of the lotus leaf.' Beilstein J Nanotechnol, 2, pp. 152-161.

Etxeberria, M., Escuin, T., Vinas, M. and Ascaso, C. (2015) 'Useful surface parameters for biomaterial discrimination.' Scanning, 37(6), pp. 429-437.

Fadeeva, E., Truong, V. K., Stiesch, M., Chichkov, B. N., Crawford, R. J., Wang, J. and Ivanova, E. P. (2011) 'Bacterial retention on superhydrophobic titanium surfaces fabricated by femtosecond laser ablation.' Langmuir, 27(6), pp. 3012-3019.

Faten, K., Hamida, K., Soumya, e. A., Saad, I. S., Hasna, M., Hassan, L. and Moktar, H. (2016) 'Lactobacillus plantarum: Effect of a protective biofilm on the surface of olives during storage.' Braz J Microbiol, 47(1), pp. 202-209.

Fister, S., Robben, C., Witte, A. K., Schoder, D., Wagner, M. and Rossmanith, P. (2016) 'Influence of Environmental Factors on Phage-Bacteria Interaction and on the Efficacy and Infectivity of Phage P100.' Front Microbiol, 7, pp. 1152.

Fontaine, B., Rault, J. and Van Oss, C. (1996) 'Microbial adhesion to solvents: a novel method to determine the electron-donor/electron-acceptor or Lewis acid-base properties of microbial cells.' Colloids and Surfaces B: Biointerfaces, 7, pp. 47-53.

Frapwell, C. J., Howlin, R. P., Soren, O., McDonagh, B. T., Duignan, C. M., Allan, R. N., Horswill, A. R., Stoodley, P., et al. (2018) 'Increased rates of genomic mutation in a biofilm co-culture model of Pseudomonas aeruginosa and Staphylococcus aureus.' bioRxiv, doi: https://DOI.org/10.1101/387233

Fu, L., Valentino, H. R. and Wand.Y. (2016) Antimicrobial food packaging. 1st ed., College of Pharmacy/School of Veterinary Sciences, University of Santiago de Compostela, Spain: Elsevier.

Gadelmawla, E., Koura, M., Maksoud, T., Elewa, I. and Soliman, H. (2002) 'Roughness parameters' Materials Processing technology, 123 pp. 133-145.

Galié, S., García-Gutiérrez, C., Miguélez, E. M., Villar, C. J. and Lombó, F. (2018) 'Biofilms in the Food Industry: Health Aspects and Control Methods.' Front Microbiol, 9, p. 898.

Giovambattista, N., Debenedetti, P. G. and Rossky, P. J. (2009) 'Enhanced surface hydrophobicity by coupling of surface polarity and topography.' Proc Natl Acad Sci USA, 106(36), pp. 15181-15185.

Gobin, M., Hawker, J., Cleary, P., Inns, T., Gardiner, D., Mikhail, A., McCormick, J., Elson, R., et al. (2018) 'National outbreak of Shiga toxin-producing.' Euro Surveill, 23(18), DOI: 10.2807/1560-7917.ES.2018.23.18.17-00197

Goh, S., Newman, C., Knowles, M., Bolton, F. J., Hollyoak, V., Richards, S., Daley, P., Counter, D., et al. (2002) 'E. coli O157 phage type 21/28 outbreak in North Cumbria associated with pasteurized milk.' Epidemiol Infect, 129(3), pp. 451-457.

Guozhen, L., Llewellyn, T., Xingxing, Z. and Jie, D. (2019) 'A review of factors affecting the efficiency of clean-in-place procedures in closed processing systems.' Energy, 178 pp. 57-71.

Gyles, C. L. (1992) 'Escherichia coli cytotoxins and enterotoxins.' Can J Microbiol, 38(7), pp. 734-746.

Hamadi, F., Latrache, H., Mabrrouki, M., Elghmari, A., Outzourhit, A., Ellouali, M. and Chtaini, A. (2005) 'Effect of pH on distribution and adhesion of Staphylococcus aureus to glass.' Journal of Adhesion Science and Technology, 19(1) pp. 73-85.

Hanson, H., Whitfield, Y., Lee, C., Badiani, T., Minielly, C., Fenik, J., Makrostergios, T., Kopko, C. (2019) 'Listeria monocytogenes Associated with Pasteurized Chocolate Milk, Ontario, Canada.' Emerg Infect Dis, 25(3), pp. 581-584.

Helbig, R., Günther, D., Friedrichs, J., Rößler, F., Lasagni, A. and Werner, C. (2016) 'The impact of structure dimensions on initial bacterial adhesion.' Biomater Sci, 4(7), pp. 1074-1078.

Huang, K., Chen, J., Nugen, S. R. and Goddard, J. M. (2016) 'Hybrid Antifouling and Antimicrobial Coatings Prepared by Electroless Co-Deposition of Fluoropolymer and Cationic Silica Nanoparticles on Stainless Steel: Efficacy against Listeria monocytogenes.' ACS Appl Mater Interfaces, 8(25), pp. 15926-15936.

Humbert, F. and Quiles, F. (2011) 'In-situ study of early stages of biofilm formation under different environmental stresses by ATR-FTIR spectroscopy.' Science against microbial pathogens.

Hwang, J., Jeong, Y., Park, J. M., Lee, K. H., Hong, J. W. and Choi, J. (2015) 'Biomimetics: forecasting the future of science, engineering, and medicine.' Int J Nanomedicine, 10, pp. 5701-5713.

Härth, M. and Schubert, D. W. (2012) 'Simple Approach for Spreading Dynamics of Polymeric Fluids.' Macromolecular Chemistry and Physics, 213(6) pp. 654-665.

Ista, L. K. and López, G. P. (2013) 'Thermodynamic analysis of marine bacterial attachment to oligo(ethylene glycol)-terminated self-assembled monolayers.' Biointerphases, 8(1), p. 24.

Jayathilake, P. G., Jana, S., Rushton, S., Swailes, D., Bridgens, B., Curtis, T. and Chen, J. (2017) 'Extracellular Polymeric Substance Production and Aggregated Bacteria Colonization Influence the Competition of Microbes in Biofilms.' Front Microbiol, 8, p. 1865.

Katsikogianni, M. and Missirlis, Y. F. (2004) 'Concise review of mechanisms of bacterial adhesion to biomaterials and of techniques used in estimating bacteria-material interactions.' Eur Cell Mater, 8, pp. 37-57.

Kesel, A. and Liedert, R. (2007) 'Learning from Nature: Non-Toxic Biofouling Control by Shark Skin Effect.' Comparative Biochemistry and Physiology, 146(4) DOI 10.1016/j.cbpa.2007.01.246

Khare, A. and Tavazoie, S. (2015) 'Multifactorial Competition and Resistance in a Two-Species Bacterial System.' PLoS Genet, 11(12), DOI:10.1371/journal.pgen.1005715

Koch, K., Bharat, B., Jung, Y. and Barthlott, W. (2008) 'Fabrication of artificial Lotus leaves and significance of hierarchical structure for superhydrophobicity and low adhesion.' Soft Matter, DOI:10.1039/B818940D

Kooten, T., Schakerraad, J., Van Der Mei, H. and Busscher, H. (1992) 'Influence of Glutaraldehyde Fixation of Cells Adherent to Solid Substrata on Their Detachment During Exposure to Shear Stress ' Cell Biophysics, 20, DOI: 10.1016/0142-9612(92)90112-2

Kyle, D. J., Oikonomou, A., Hill, E., Vijayaraghavan, A. and Bayat, A. (2016) 'Fabrication and modelling of fractal, biomimetic, micro and nano-topographical surfaces.' Bioinspir Biomim, 11(4) DOI: 10.1088/1748-3190/11/4/046009

Lancashire, H. (2017) 'A simulated comparison between profile and areal surfaceparameters: Ra as an estimate of Sa.'

Law, K. (2014) 'Definitions for Hydrophilicity, Hydrophobicity, and Superhydrophobicity: Getting the Basics Right.' American Chemical Society, 4(5) pp. 686-688.

Lazzini, G., Romoli, L., Lutey, A. and Fuso, F. (2019) 'Modelling the interaction between bacterial cells and laser-textured surfaces.' Surface Coatings Technology, 375, pp. 8-14.

Lee, L. (1996) 'Correlation between Lewis Acid-Base Surface Interaction Components and Linear Solvation Energy Relationship Solvatochromic α and β Parameters.' Langmuir, 12, pp. 1681-1687.

Lim, J. Y., Yoon, J. and Hovde, C. J. (2010) 'A brief overview of Escherichia coli O157:H7 and its plasmid O157.' J Microbiol Biotechnol, 20(1), pp. 5-14.

Lorenzetti, M., Dogša, I., Stošicki, T., Stopar, D., Kalin, M., Kobe, S. and Novak, S. (2015) 'The influence of surface modification on bacterial adhesion to titanium-based substrates.' ACS Appl Mater Interfaces, 7(3), pp. 1644-1651.

Madsen, J. S., Burmølle, M., Hansen, L. H. and Sørensen, S. J. (2012) 'The interconnection between biofilm formation and horizontal gene transfer.' FEMS Immunol Med Microbiol, 65(2), pp. 183-195.

Magin, C. M., Neale, D. B., Drinker, M. C., Willenberg, B. J., Reddy, S. T., La Perle, K. M., Schultz, G. S. and Brennan, A. B. (2016) 'Evaluation of a bilayered, micropatterned hydrogel dressing for full-thickness wound healing.' Exp Biol Med, 241(9), pp. 986-995.

Mao, Y., Kumar, P., Subramanian, K., Tawfiq, K. and Chen, G. (2011) 'Microbial Biofouling: A Mechanistic Investigation.' Journal of adhesion science and technology, 25 pp. 2155-2168.

Marcell, L. M. and Beattie, G. A. (2002) 'Effect of leaf surface waxes on leaf colonization by Pantoea agglomerans and Clavibacter michiganensis.' Mol Plant Microbe Interact, 15(12), Dec, pp. 1236-1244.

Marmur, A. (2003) 'Wetting on Hydrophobic Rough Surfaces: To Be Heterogeneous or Not To Be?' Langmuir, 19 pp. 8343-8348.

Marsh, P. D., Moter, A. and Devine, D. A. (2011) 'Dental plaque biofilms: communities, conflict and control.' Periodontol 2000, 55(1), pp. 16-35.

Marshall, K. C. (1986) 'Adsorption and adhesion processes in microbial growth at interfaces.' Adv Colloid Interface Sci, 25(1), pp. 59-86.

McClure, P. J. and Hall, S. (2000) 'Survival of Escherichia coli in foods.' Symp Ser Soc Appl Microbiol, (29) pp. 61S-70S.

Mellefont, L. A., McMeekin, T. A. and Ross, T. (2008) 'Effect of relative inoculum concentration on Listeria monocytogenes growth in co-culture.' Int J Food Microbiol, 121(2), pp. 157-168.

Mitik-Dineva, N., Wang, J., Mocanasu, R. C., Stoddart, P. R., Crawford, R. J. and Ivanova, E. P. (2008) 'Impact of nano-topography on bacterial attachment.' Biotechnol J, 3(4), pp. 536-544.

Najafinobar, N. (2011) 'Effect of nanotopography on bacterial adhesion and EPS production (unpublished master's thesis). Chalmers Institute of Technology, Gothenberg Sweden.

Nejadnik, M. R., van der Mei, H. C., Busscher, H. J. and Norde, W. (2008) 'Determination of the shear force at the balance between bacterial attachment and detachment in weak-adherence systems, using a flow displacement chamber.' Appl Environ Microbiol, 74(3), pp. 916-919.

Palmer, J., Flint, S. and Brooks, J. (2007) 'Bacterial cell attachment, the beginning of a biofilm.' J Ind Microbiol Biotechnol, 34(9), pp. 577-588.

Park, A., Jeong, H., Lee, J., Kim, K. and Lee, C. (2011) 'Effect of shear stress on the formation of bacterial biofilm in a microfluidic channel.' BioChip Journal, 5(3) pp. 236-241.

Peeters, E., Nelis, H. J. and Coenye, T. (2008) 'Comparison of multiple methods for quantification of microbial biofilms grown in microtiter plates.' J Microbiol Methods, 72(2), pp. 157-165.

Pennington, T. H. (2014) 'E. coli O157 outbreaks in the United Kingdom: past, present, and future.' Infect Drug Resist, 7, pp. 211-222.

Pereni, C. I., Zhao, Q., Liu, Y. and Abel, E. (2006) 'Surface free energy effect on bacterial retention.' Colloids Surf B Biointerfaces, 48(2), pp. 143-147.

Perera-Costa, D., Bruque, J. M., González-Martín, M. L., Gómez-García, A. C. and Vadillo-Rodríguez, V. (2014) 'Studying the influence of surface topography on bacterial adhesion using spatially organized microtopographic surface patterns.' Langmuir, 30(16), pp. 4633-4641.

Pizarro-Cerda, J. and Cossart, P. (2006) 'Bacterial Adhesion and Entry into Host Cells.' Cell, 124(4) pp. 715-727.

Pringle, J. H. and Fletcher, M. (1983) 'Influence of substratum wettability on attachment of freshwater bacteria to solid surfaces.' Appl Environ Microbiol, 45(3), pp. 811-817.

Rajab, F. H., Liauw, C. M., Benson, P. S., Li, L. and Whitehead, K. A. (2017) 'Production of hybrid macro/micro/nano surface structures on Ti6Al4V surfaces by picosecond laser surface texturing and their antifouling characteristics.' Colloids Surf B Biointerfaces, 160, pp. 688-696.

Ramaswamy, V., Cresence, V. M., Rejitha, J. S., Lekshmi, M. U., Dharsana, K. S., Prasad, S. P. and Vijila, H. M. (2007) 'Listeria--review of epidemiology and pathogenesis.' J Microbiol Immunol Infect, 40(1), pp. 4-13.

Reddy, S. T., Chung, K. K., McDaniel, C. J., Darouiche, R. O., Landman, J. and Brennan, A. B. (2011) 'Micropatterned surfaces for reducing the risk of catheter-associated urinary tract infection: an in vitro study on the effect of sharklet micropatterned surfaces to inhibit bacterial colonization and migration of uropathogenic Escherichia coli.' J Endourol, 25(9), pp. 1547-1552.

Reichhardt, C. and Parsek, M. R. (2019) 'Confocal Laser Scanning Microscopy for Analysis of.' Front Microbiol, p. 677.

Rosairo, O., Azeredo, J., Teixeira, P. and Fonseca, A. (2001) 'The role of hydrophobicity in bacterial adhesion.' Hydrophobicity and Adhesion, 5 pp. 11-22.

Rosenberg, M. (2006) 'Microbial adhesion to hydrocarbons: twenty-five years of doing MATH.' Federation of European Microbiological Societies, 262, pp. 129-134.

Scardino, A. J., Hudleston, D., Peng, Z., Paul, N. A. and de Nys, R. (2009) 'Biomimetic characterisation of key surface parameters for the development of fouling resistant materials.' Biofouling, 25(1) pp. 83-93.

Schumacher, J. F., Long, C. J., Callow, M. E., Finlay, J. A., Callow, J. A. and Brennan, A. B. (2008) 'Engineered nanoforce gradients for inhibition of settlement (attachment) of swimming algal spores.' Langmuir, 24(9), pp. 4931-4937.

Segado-Arenas, A., Atienza-Cuevas, L., Broullón-Molanes, J. R., Rodríguez-González, M. and Lubián-López, S. P. (2018) 'Late stillbirth due to listeriosis.' Autops Case Rep, 8(4), DOI:10.4322/acr.2018.051

Shahali, H., Hasan, J., Mathews, A., Wang, H., Yan, C., Tesfamichael, T. and Yarlagadda, P. (2019) 'Multi-biofunctional properties of three species of cicada wings and biomimetic fabrication of nanopatterned titanium pillars.' Journal of Materials Chemistry B, 7(8), pp. 1300-1310

Sharpe. (2011) Time For HVLP. Support. Graco. [Online] [Accessed on 14/10/2019] http://www.sharpe1.com/sharpe/sharpe.nsf/Page/Time+For+HVLP

Singh, A. V., Vyas, V., Patil, R., Sharma, V., Scopelliti, P. E., Bongiorno, G., Podestà, A., Lenardi, C., et al. (2011) 'Quantitative characterization of the influence of the nanoscale

morphology of nanostructured surfaces on bacterial adhesion and biofilm formation.' PLoS One, 6(9) DOI:10.1371/journal.pone.0025029

Siriratruengsuk, W., Siriratruengsuk, W., Furuuchi, M., Prueksasit, T. and Ekawan, L. (2017) 'Potential of Pyrene Removal from Urban Environments by the Activities of Bacteria and Biosurfactant on Ornamental Plant Leaves.' Water, Air, & Soil Pollution, 228(264), p.264

Song, F., Koo, H. and Ren, D. (2015) 'Effects of Material Properties on Bacterial Adhesion and Biofilm Formation.' J Dent Res, 94(8), pp. 1027-1034.

Tripathy, A., Sen, P., Su, B. and Briscoe, W. H. (2017) 'Natural and bioinspired nanostructured bactericidal surfaces.' Adv Colloid Interface Sci, 248, pp. 85-104.

Vaidya, N. and Solgaard, O. (2018) '3D printed optics with nanometer scale surface roughness. 'Microsyst Nanoeng, 4, p.18.

Van Oss, C. J. (1995) 'Hydrophobic, hydrophilic and other interactions in epitope-paratope binding.' Mol Immunol, 32(3), pp. 199-211.

Whitehead, K. and Verran, J. (2006) 'The effect of surface topography on the retention of microorganisms.' Food and Bioproducts Processing, 84(4) pp. 253-259.

Whitehead, K. and Verran, J. (2015) 'Formation, architecture and functionality of microbial biofilms in the food industry.' Current opinion in food science, 2, pp.84-91.

Whitehead, K. A., Olivier, S., Benson, P. S., Arneborg, N., Verran, J. and Kelly, P. (2015) 'The effect of surface properties of polycrystalline, single phase metal coatings on bacterial retention.' Int J Food Microbiol, 197, pp. 92-97.

Wickens, D., Lynch, S., West, G., Kelly, P., Verran, J. and Whitehead, K. A. (2014) 'Quantifying the pattern of microbial cell dispersion, density and clustering on surfaces of differing chemistries and topographies using multifractal analysis.' J Microbiol Methods, 104, pp. 101-108.

Wiedemeier, S., Wächter, S. and Kolbe, C. (2017) 'Precision moulding of biomimetic disposable chips for droplet-based applications.' Microfluidics and Nanofluidics, 21, DOI:10.1007/s10404-017-2005-5

Wu, S., Altenried, S., Zogg, A., Zuber, F., Maniura-Weber, K. and Ren, Q. (2018) 'Role of the Surface Nanoscale Roughness of Stainless Steel on Bacterial Adhesion and Microcolony Formation.' ACS Omega, 3(6), pp. 6456-6464.

Wullt, B. (2003) 'The role of P fimbriae for Escherichia coli establishment and mucosal inflammation in the human urinary tract.' Int J Antimicrob Agents, 21(6), pp. 605-621.

Xiao, M., Yang, H., Xiao, Q., Zhang, H. and Chen, X. (2019) 'Decentralized manufacturing for biomimetics through cooperation of digitization and nanomaterial design.' Nanoscale, 11(41), pp. 19179-19189.

Yamamoto, M., Nishikawa, N., Mayama, H., Nonomura, Y., Yokojima, S., Nakamura, S. and Uchida, K. (2015) 'Theoretical Explanation of the Lotus Effect: Superhydrophobic Property Changes by Removal of Nanostructures from the Surface of a Lotus Leaf.' Langmuir, 31(26), pp. 7355-7363.

Yannopapas, V. and Vitanov, N. V. (2007) 'First-principles theory of van der Waals forces between macroscopic bodies.' Phys Rev Lett, 99(12), p. 120406.

Yuan, Y., Hays, M., Hardwidge, P. and Kim, J. (2017) 'Surface characteristics influencing bacterial adhesion to polymeric substrates.' Royal society of chemistry, 7, pp. 14254-14261.

Zeisler-Diehl, V. V., Barthlott, W. and Schreiber, L. (2018) 'Plant Cuticular Waxes: Composition, Function, and Interactions with Microorganisms.' Hydrocarbons, Oils and Lipids: Diversity, Origin, Chemistry and Fate' doi:10.1007/978-3-319-54529-5_7-1

Zhang, X., Zhang, Q., Yan, T., Jiang, Z. and Zuo, Y. Y. (2015) 'Quantitatively predicting bacterial adhesion using surface free energy determined with a spectrophotometric method.' Environ Sci Technol, 49(10), pp. 6164-6171.